

**<sup>14</sup>C reservoir ages  
and oceanic carbon  
storage**

M. Sarnthein et al.

# Peak glacial<sup>14</sup>C ventilation ages suggest major draw-down of carbon into the abyssal ocean

M. Sarnthein<sup>1,3,\*</sup>, B. Schneider<sup>1,\*</sup>, and P. M. Grootes<sup>2,\*</sup>

<sup>1</sup>Institut für Geowissenschaften, University of Kiel, Olshausenstr. 40, 24098 Kiel, Germany

<sup>2</sup>Leibniz Laboratory, University of Kiel, Olshausenstr. 40, 24098 Kiel, Germany

<sup>3</sup>Institut für Geologie und Paläontologie, University of Innsbruck, Innsbruck, Austria

\* These authors contributed equally to this work.

Received: 31 January 2013 – Accepted: 1 February 2013 – Published: 13 February 2013

Correspondence to: M. Sarnthein (ms@gpi.uni-kiel.de)

Published by Copernicus Publications on behalf of the European Geosciences Union.

Title Page

Abstract

Introduction

Conclusions

References

Tables

Figures

⏪

⏩

◀

▶

Back

Close

Full Screen / Esc

Printer-friendly Version

Interactive Discussion



## Abstract

Ice core records demonstrate a glacial-interglacial atmospheric CO<sub>2</sub> increase of ~ 100 ppm. A transfer of ~ 530 GtC is required to produce the deglacial rise of carbon in the atmosphere and terrestrial biosphere. This amount is usually ascribed to oceanic carbon release, although the actual mechanisms remained elusive, since an adequately old and carbon-enriched deep-ocean reservoir seemed unlikely. Here we present a new, though still fragmentary, ocean-wide <sup>14</sup>C dataset showing that during the Last Glacial Maximum (LGM) and Heinrich Stadial 1 (HS-1) the <sup>14</sup>C age difference between ocean deep waters and the atmosphere exceeded the modern values by up to 1500 <sup>14</sup>C yr, in the extreme reaching 5100 yr. Below 2000 m depth the <sup>14</sup>C ventilation age of modern ocean waters is directly linked to the concentration of dissolved inorganic carbon (DIC). We assume that the range of regression slopes of DIC vs. Δ<sup>14</sup>C remained constant for LGM times, which implies that an average LGM aging by ~ 600 <sup>14</sup>C yr corresponded to a global rise by ~ 85–115 μmol DIC kg<sup>-1</sup> in the deep ocean. Thus, the prolonged residence time of ocean deep waters indeed made it possible to absorb an additional ~ 730–980 Gt DIC, ~ 1/3 of which transferred from intermediate waters. We infer that LGM deep-water O<sub>2</sub> dropped to suboxic values of < 10 μmol kg<sup>-1</sup> in the Atlantic sector of the Southern ocean, possibly also in the subpolar North Pacific. The transfer of aged deep-ocean carbon to the atmosphere and the ocean-atmosphere exchange are sufficient to account for the 190-‰ drop in atmospheric <sup>14</sup>C during the so-called HS-1 “Mystery Interval”.

## 1 Introduction

Global climatic and oceanic conditions underwent a series of fundamental transitions after the Last Glacial Maximum (LGM) ended near 19 ka (Mix et al., 2001). These transitions supposedly comprised conflicting trends on land and in the ocean, which are difficult to reconcile. In particular, this applies to the North Atlantic meltwater

CPD

9, 925–965, 2013

## <sup>14</sup>C reservoir ages and oceanic carbon storage

M. Sarnthein et al.

Title Page

Abstract

Introduction

Conclusions

References

Tables

Figures



Back

Close

Full Screen / Esc

Printer-friendly Version

Interactive Discussion



stadial Heinrich 1 (HS-1), 17.5–14.7 ka, hence named “Mystery Interval” (Denton et al., 2006; Broecker and Barker, 2007) over which the atmospheric  $^{14}\text{C}$  level decreased by  $\sim 190\text{‰}$ .

Notably, there is conflicting evidence about the whereabouts of carbon during the LGM and the potential low- $^{14}\text{C}$  sources for the significant deglacial rise in atmospheric and terrestrial carbon by 200 Gt (Monnin et al., 2001) and 330–500 Gt (Ciais et al., 2012), respectively. This problem is directly tied to questions regarding the state of the LGM deep ocean, the largest carbon reservoir of the surface Earth systems, and the fundamental deglacial changes in ocean circulation that may have influenced it. These changes have substantially controlled the ocean’s capacity to store carbon.

Theoretical considerations and first evidence clearly suggest an enhanced LGM storage of carbon in the abyssal ocean (Archer and Winguth, 2000; Broecker, 1982; Bryan et al., 2010; Yu et al., 2010). However, box model results (Hain et al., 2010) and rough calculations on the basis of first abyssal ventilation ages (Broecker and Barker, 2007) suggested a series of potential major shortcomings in the concept that claims a reduced glacial Meridional Overturning Circulation (MOC) caused enhanced LGM storage. Thus the concept was rejected as quantitatively unreasonable in terms of radio-carbon budgets.

On the basis of box model experiments Skinner (2009) proposed an expanded LGM volume of relatively cold and carbon-enriched deep waters analogous to the modern Circumpolar Deepwater. This mechanism would lead to an enlarged marine carbon inventory, supposedly without requiring “pre-imposed (deglacial) changes in (deep) ocean overturning rate”. In contrast, we now present an approach that assumes changing characteristics of deep waters in a constant ocean volume.

Modern  $^{14}\text{C}$  ventilation ages (Matsumoto, 2007) (Fig. 1) depict a clear pattern of the sources and centennial-scale directions in the circulation of the abyssal ocean, that is the basis for the concept of an “ocean salinity conveyor belt” which starts from the northern North Atlantic and terminates in the North Pacific after almost 2000 yr (Stommel, 1961; Broecker, 1991). To test the various model postulates and suggestions for

CPD

9, 925–965, 2013

## $^{14}\text{C}$ reservoir ages and oceanic carbon storage

M. Sarnthein et al.

Title Page

Abstract

Introduction

Conclusions

References

Tables

Figures



Back

Close

Full Screen / Esc

Printer-friendly Version

Interactive Discussion



---

## <sup>14</sup>C reservoir ages and oceanic carbon storage

M. Sarnthein et al.

---

Title Page

Abstract

Introduction

Conclusions

References

Tables

Figures



Back

Close

Full Screen / Esc

Printer-friendly Version

Interactive Discussion



past changes in the carbon budget of the global ocean, we now employ a set of modern and past apparent <sup>14</sup>C ventilation ages for ocean deep waters below 1500 m/2000 m water depth (w.d.) (Bard, 1998; Sarnthein, 2011; detailed data sources in Table 1b). By comparison with previous related studies (Campin et al., 1999), our data set is much enlarged and more robust. Moreover, it stays below the fairly complex “pipeline” system characteristic of intermediate-water circulation (Burke and Robinson, 2012), hence promises an improved understanding of the glacial-to-deglacial changes in the carbon inventory of the abyssal ocean.

As shown in the subsequent section on “Modern linkages etc.” and Fig. 2a, our approach rests essentially on the largely linear relationship between modern ventilation ages and modern concentrations of dissolved inorganic carbon (DIC) in the deep ocean below > 2000 m w.d. (GLODAP data; Key et al., 2004). Having constrained its uncertainty range (Fig. 2b) extrapolation enables us to estimate tentatively the scope of the glacial-to-deglacial redistribution of carbon inventories on the basis of coeval shifts in the average ventilation age of deepwaters (Fig. 3). In particular, we test the LGM scenario and compare it with that of HS-1 and the warm Bølling-Allerød (B/A) interstadial. The resulting shifts in the DIC concentration of the abyssal ocean are compared with patterns deduced from other proxies such as B/Ca records (Yu et al., 2010) and with the early deglacial drop in atmospheric  $\Delta^{14}\text{C}$  by  $190 \pm 10\text{‰}$  over HS-1 (Broecker and Barker, 2007).

Past changes in the ventilation age of the abyssal ocean also enable us to draw preliminary conclusions on deglacial changes in the source, intensity, and global directions of ocean MOC (Rahmstorf, 2006), changes to be reconciled with independent evidence from other proxies such as benthic  $\delta^{13}\text{C}$  (McCave et al., 2008; Sarnthein et al., 1994), Pa/Th (Negre et al., 2010), and Nd records (Basak et al., 2010).



4–6, we do employ the interpolated modern deep-water ventilation age shown in the gridded-data map of Matsumoto (2007) to derive the age anomalies between LGM, HS-1, B/A, and today for each core site listed in Table 1 by means of simple comparison with the reconstructed ventilation age estimate.

## 2.2 Solubility pump and preformed carbon: modern vs. past

The deep-ocean carbon reservoir is fed by the “solubility pump” plus “preformed” carbon, initially dissolved and downwelled by juvenile deep waters from the ocean surface and atmosphere (Raven and Falkowski, 1999; Sigman et al., 2010), later on by the “biological pump”, that is the export flux of particulate organic and inorganic biogenic carbon from the surface ocean (Schlitzer, 2002). The input of preformed carbon plus solubility pump is ten times larger than that of the biological pump, as documented by an initial concentration of  $\sim 2165 \mu\text{molCkg}^{-1}$  sea water in the source region of North Atlantic Deepwater (NADW) (Fig. 2a), a source that clearly dominates the abyssal carbon inventory. By contrast, the gradual, almost linear rise of DIC (summing up to  $\sim 220 \mu\text{molCkg}^{-1}$  over 2400  $^{14}\text{C}$  yr) and  $^{14}\text{C}$  ventilation ages of deep waters with increasing distance from their source is determined by a delicate balance between the gradual aging of preformed carbon and an ongoing input of young carbon supplied by the biological pump from the sea surface.

Close to the minimum ventilation age of 400–600 yr the regression of dissolved carbon vs. ventilation age extends into a long “horizontal tail” (Fig. 2a). This tail is located in the North Atlantic on the downwelling branch of NADW, at sites where the exchange of carbon between atmosphere and deep ocean is particularly fast. Moreover, a closer look at the regression reveals a small but distinct “bump”, that is a small number of positive outliers in DIC (total carbon) at reduced  $^{14}\text{C}$  age, which deviate from the general regression slope near  $-135 \text{‰} \Delta^{14}\text{C}$ . These anomalies may facilitate our understanding of (1) the processes that control the gradual increase in apparent  $^{14}\text{C}$  ventilation ages and (2) the potential to extrapolate the  $^{14}\text{C}$ –DIC relationship of Fig. 2 to climatic scenarios in the past. Both anomalies match an enhanced concentration of

CPD

9, 925–965, 2013

## $^{14}\text{C}$ reservoir ages and oceanic carbon storage

M. Sarnthein et al.

Title Page

Abstract

Introduction

Conclusions

References

Tables

Figures

⏪

⏩

◀

▶

Back

Close

Full Screen / Esc

Printer-friendly Version

Interactive Discussion



chlorofluorocarbons (CFC11;  $> 0.1 \text{ pmol kg}^{-1}$  sea water) that clearly trace the modern anthropogenic influence, thus also mark an increased uptake of anthropogenic carbon which needs to be ignored. The bump in the regression slope near  $-135\text{‰}$   $^{14}\text{C}$  is confined to a narrow longitudinal range between  $\sim 20^\circ\text{W}$  and  $30^\circ\text{E}$  in the South Atlantic, precisely the region, where modern Weddell Sea Bottom Water (WSBW) is mixing with NADW and Circumpolar Water (CPW) in the Southern Ocean (Matsumoto, 2007). The admixed WSBW conveys additional  $^{14}\text{C}$  from a more recent, though weak, contact with the atmosphere, thus having lower  $^{14}\text{C}$  ages than the NADW after  $> 700$  yr of circulation. Accordingly, the admixture results in a slight rejuvenation of CPW and an increased level of preformed carbon. This marks these waters continuously as long as they flow farther east into the Indo-Pacific, hence induces a slight upward shift of the fairly robust regression slope in Fig. 2a. A further source of  $^{14}\text{C}$  may be located in the Ross Sea,  $170^\circ\text{--}180^\circ\text{E}$ . However, CFC data from this region (Orsi et al., 2002) indicate an only marginal contribution of anthropogenically affected, hence very young  $\text{CO}_2$ , which we regard as negligible.

Different from the conjecture of Campin et al. (1999), the downwelling of deep waters from the Weddell Sea does not lead to DIC depletion of circumpolar and Pacific deep waters, rather to a slight and partly anthropogenic (Mikaloff-Fletcher et al., 2006) enrichment in DIC. Probably, this unexpected trend results from the short time, during which the upwelled waters are exposed to the atmosphere prior to their renewed downwelling in the circum-Antarctic polynyas. This interval is too short for a major carbon release after equilibration of the carbonate system with the atmosphere since the reaction among the different species of the marine carbonate system is slow (Sigman and Boyle, 2000). Per theory, an equilibrium between atmospheric and surface ocean  $p\text{CO}_2$  requires an open contact over about six months (Sarmiento and Gruber, 2006). Seasonally open polynyas in the Weddell Sea region are lasting for six months and less. Thus the exchange of  $\text{CO}_2$  with the atmosphere will rejuvenate only less than 50 % of carbon-enriched NADW waters upwelled over a whole year, which in turn leads to an initial age of  $< \sim 1200$  yr of Weddell Sea Deepwater. Probably, the exposure time would

CPD

9, 925–965, 2013

## $^{14}\text{C}$ reservoir ages and oceanic carbon storage

M. Sarnthein et al.

Title Page

Abstract

Introduction

Conclusions

References

Tables

Figures



Back

Close

Full Screen / Esc

Printer-friendly Version

Interactive Discussion



not rise, rather drop, with a much increased circum-Antarctic sea ice cover during peak glacial times (Gersonde et al., 2003).

To assess the storage capacity of DIC in the LGM abyssal ocean, we first roughly estimate past changes in the minimum level of the “solubility pump plus preformed carbon”, today contributing  $2165 \mu\text{mol C kg}^{-1}$  at the main regions of peak glacial deep-water formation in the North Atlantic, the Labrador and Norwegian Seas. These estimates consider the joint effect of a peak-glacial drop in atmospheric  $\text{CO}_2$  by 30% (Monnin et al., 2001), a  $3^\circ\text{C}$  drop in glacial SST (based on census counts of planktic foraminifera; Pflaumann et al., 2003), a contemporaneous 1-psu rise in sea surface salinity (based on census counts and  $\delta^{18}\text{O}$  records of planktic foraminifera; Duplessy et al., 1991a), and a slightly elevated alkalinity (+3%; as the result of increased salinity and enhanced cation concentrations due to lowered sea level), following widely accepted LGM proxy data such as benthic  $\delta^{13}\text{C}$  transects (Sarnthein et al., 1994). Counter-intuitively, the outlined variations of boundary conditions induce little change, hardly exceeding 3 per mil of the total carbon mass ascribed to preformed DIC.

### 2.3 Transfer functions: caveats and solutions

To establish transfer functions for deducing past concentrations of DIC, alkalinity, oxygen, and  $\text{PO}_4$  in the deep ocean from measured  $^{14}\text{C}$  concentrations, modern ventilation ages of deep waters were compared with modern concentrations of DIC, alkalinity,  $\text{O}_2$ , and  $\text{PO}_4$  in the abyssal ocean below 2000 m w.d. (GLODAP data; Key et al., 2004; Table 1). In our text we only refer to stoichiometric principles as far as they concern the gradients of our age–organic-carbon derived DIC, age–alkalinity, age–oxygen, and age– $\text{PO}_4$  relationships. We use the slopes of organic carbon (derived from potential alkalinity) vs. age and oxygen vs. age to calculate the organic carbon ( $\text{C}_{\text{org}}$ )/oxygen ratio of respiration. Although not of major importance to the findings of this study, this test provides a simple check of consistency. Values vary from 0.48–1.43 for the different ocean basins and give a global average  $\text{C}_{\text{org}}/\text{O}_2$  respiration ratio of 0.95. These values agree reasonably well with averages of 1.13 and 1.23–1.7, published by Redfield

CPD

9, 925–965, 2013

## $^{14}\text{C}$ reservoir ages and oceanic carbon storage

M. Sarnthein et al.

Title Page

Abstract

Introduction

Conclusions

References

Tables

Figures

◀

▶

◀

▶

Back

Close

Full Screen / Esc

Printer-friendly Version

Interactive Discussion



## <sup>14</sup>C reservoir ages and oceanic carbon storage

M. Sarnthein et al.

Title Page

Abstract

Introduction

Conclusions

References

Tables

Figures



Back

Close

Full Screen / Esc

Printer-friendly Version

Interactive Discussion



et al. (1963) and Takahashi et al. (1985), respectively. However,  $C_{\text{org}}/\text{PO}_4$  ratios estimated from the slopes of  $C_{\text{org}}$  and  $\text{PO}_4$  versus age reveal generally low values of 45–109 and a global average of 80, as compared to published values of 103–122. Yet, respective uncertainties are probably large due to low slope gradients of generally low concentrations in  $\text{PO}_4$ .

Modern  $^{14}\text{C}$  ventilation ages increase from about 600 up to 2400 yr with increasing distance from the deep-water source. This aging of deep waters by 1800 yr matches an increase by  $230 \mu\text{mol DIC kg}^{-1}$  sea water at the terminus of the conveyor belt in the Pacific, on average  $1.22 \mu\text{mol DIC kg}^{-1}$  per 1‰ decrease in  $^{14}\text{C}$ . Since an average concentration of  $1 \mu\text{mol DIC kg}^{-1}$  corresponds to 8.5 Gt C in the deep ocean volume here considered (based on ETOPO-60; Amante and Eakins, 2009, and GLODAP data), this implies that the modern abyssal ocean is picking up almost  $1.1 \text{ Gt C yr}^{-1}$ . As shown below, this carbon uptake is assigned to the “biological pump” that incorporates  $0.64 \text{ Gt C yr}^{-1}$  from remineralized particulate organic matter (POC) plus  $0.45 \text{ Gt C yr}^{-1}$  from the dissolution of calcium carbonate (PIC). In total, the organic carbon flux below 2000 m depth covers a narrow range of variability near 6% of the export flux from the surface ocean (Schlitzer, 2002), thus comes close to independent estimates (Antia et al., 2001).

The separation of the organic and inorganic (calcite) contribution to the deep-ocean DIC increase is inferred from the regression of  $\Delta^{14}\text{C}$  versus potential alkalinity. POTALK is the sum of total alkalinity and nitrate, normalized to salinity, and shows the influence of  $\text{CaCO}_3$  dissolution on total alkalinity. Accordingly, a 1‰ decrease in  $\Delta^{14}\text{C}$  parallels an increase of 1 (0.8–1.7)  $\mu\text{mol kg}^{-1}$  POTALK (Fig. 4). Due to the 2 : 1 relationship of alkalinity versus DIC changes under  $\text{CaCO}_3$  precipitation/dissolution (Zeebe and Wolf-Gladrow, 2001), a  $1 \mu\text{mol kg}^{-1}$  rise in POTALK contributes  $0.5 \mu\text{mol kg}^{-1}$  DIC to a total increase of  $1.22 \mu\text{mol kg}^{-1}$  DIC per 1‰ decrease in  $\Delta^{14}\text{C}$ . The remainder of  $0.72 \mu\text{mol kg}^{-1}$  represents the actual organic carbon contribution. Assuming an average aging of the water masses by 9.7 yr per 1‰ decrease in  $\Delta^{14}\text{C}$ , the rate of total carbon remineralization in the deep ocean amounts to  $0.64 \text{ Gt C yr}^{-1}$  stemming from particulate

organic carbon (POC) and  $0.45 \text{ GtCyr}^{-1}$  coming from calcite dissolution (particulate inorganic carbon = PIC).

The outlined gross fluxes of POC and PIC, possibly in combination with a slower but prolonged remineralization of POC, may have varied over the past due to changes in both  $\text{NO}_3$  of surface waters and the “rain ratio” between organic and carbonate carbon (Berger and Keir, 1984), leaving an imprint on the alkalinity of deep waters (Fig. 4). This hinders any simple extrapolation of the modern average DIC-age ratio of  $-1.22 \mu\text{mol}\%^{-1} \text{ }^{14}\text{C}$  to past climatic scenarios. In its direct form we cannot solve this question for a lack of data. However, we may use a probability argument that is based on a test of the variability of the DIC-age relationship over six major basins in the modern ocean (Fig. 5).

Accordingly, the regression slopes of the four largest ocean basins range from  $-1.27$  to  $-1.49 \mu\text{molDIC}\%^{-1} \text{ }^{14}\text{C}$  (Fig. 2b). The far northwestern Indian Ocean forms an exception with  $-1.87 \mu\text{mol}\%^{-1} \text{ }^{14}\text{C}$ , which is controlled by upwelling productivity in the Arabian Sea. This is an unlikely large-scale analogue for the glacial ocean and is hence ignored. In contrast, a much lower ratio of  $-0.79 \mu\text{mol}\%^{-1} \text{ }^{14}\text{C}$  is characteristic of the southern South Pacific (Fig. 5), and might be an analogue for some glacial and deglacial basins. East of Australia the modern ocean shows a major eastward decrease in the (dust-borne) nutrient supply. Thus, both carbon flux and  $\text{PO}_4$ -age ratio are four times lower in the Pacific sector than in the Atlantic and Indian sectors of the Southern Ocean (Table 1). Yet, this decrease did not necessarily apply to the LGM, when enlarged Patagonian and Australian deserts in combination with increased storminess led to a significant rise in the flux of dust and iron to the southern South Pacific, in particular north of  $50\text{--}60^\circ \text{S}$  (Thiede, 1979). Thus we may assume that the (de)glacial productivity in this region was more similar to that further west and that the overall glacial variability of the gradient in the DIC-age ratio did hardly exceed the modern range of  $-1.25$  to  $-1.5 \mu\text{molDIC per kg seawater and } \% \text{ }^{14}\text{C}$ , although somewhat differently distributed.

## $^{14}\text{C}$ reservoir ages and oceanic carbon storage

M. Sarnthein et al.

Title Page

Abstract

Introduction

Conclusions

References

Tables

Figures



Back

Close

Full Screen / Esc

Printer-friendly Version

Interactive Discussion



## <sup>14</sup>C reservoir ages and oceanic carbon storage

M. Sarnthein et al.

Title Page

Abstract

Introduction

Conclusions

References

Tables

Figures



Back

Close

Full Screen / Esc

Printer-friendly Version

Interactive Discussion



In summary, this variability test suggests that the range of differential regression slopes which characterize sea regions 1–6 (listed in Fig. 2b and Table 1) serves as adequate basis to estimate DIC values for the widest–possible range of scenarios of the biological pump in the modern deep ocean. Thus we may employ this range for extrapolation to past scenarios, since the global nutrient input and bulk biological pump may then have been controlled by basically similar conditions as today. Note, this extrapolation does not apply to intermediate waters not addressed in our study.

Our working hypothesis to extrapolate the modern average regression slope will need to be tested for LGM conditions by means of a general circulation model (GCM) simulation that couples changes in climate and the carbon cycle. However, all GCM runs presently available suffer from a lack of general consensus on the properly modeled circulation patterns that apply for the LGM (Tagliabue et al., 2009) and/or from deficits in carbon mass conservation. Also, an important boundary condition for any model test, the robustness of the C : N : P element ratios resulting from organic particle remineralization (Redfield et al., 1963), appears questionable (Schneider, 2003).

### 3 Estimates of past deep-ocean <sup>14</sup>C reservoir ages – methods and sources

Robust estimates for (apparent) <sup>14</sup>C paleoventilation ages of deep waters at > 1500 m depth are derived from marine sediment records by means of five different techniques (1) paired U/Th- and <sup>14</sup>C-based age estimates of deep-water corals (Adkins et al., 1998; Robinson et al., 2005; LGM uncertainty range of ± ~ 500 yr); (2) the <sup>14</sup>C “projection method” applied to <sup>14</sup>C ages measured on benthic foraminifers (Marchitto et al., 2007; Franke et al., 2008; Barker et al., 2010; LGM uncertainty range up to > ± 600 yr); absolute-age estimates for planktic and benthic <sup>14</sup>C ages that are deduced (3) from tephrochronology (Rose et al., 2010; Thornalley et al., 2011; centennial-scale uncertainty range) or (4) by means of high-resolution tuning of marine climate records to the elaborate, in part annual-layer-based chronology of nearby ice core records (Thornalley et al., 2011; Skinner et al., 2010; estimated LGM uncertainty range: 300–1000 yr);

**$^{14}\text{C}$  reservoir ages and oceanic carbon storage**

M. Sarnthein et al.

[Title Page](#)[Abstract](#)[Introduction](#)[Conclusions](#)[References](#)[Tables](#)[Figures](#)[Back](#)[Close](#)[Full Screen / Esc](#)[Printer-friendly Version](#)[Interactive Discussion](#)

and (5) the  $^{14}\text{C}$  plateau tuning technique (Sarnthein et al., 2007; further details in Sarnthein et al., 2011; estimated LGM uncertainty range of  $\pm 250$ – $450$  yr). This technique derives past reservoir ages of surface waters from the excess age of  $^{14}\text{C}$  plateaus in planktic foraminiferal  $^{14}\text{C}$  records over the ages of a suite of up to 7 well constrained atmospheric  $^{14}\text{C}$  plateaus during Termination 1 (ages in Table 1a were modified on the basis of the “Suigetsu Record” of Ramsey et al., 2012). The age-defined upper and lower plateau boundaries provide absolute age estimates. Planktic reservoir ages plus the age difference between paired benthic and planktic  $^{14}\text{C}$  data provide deep-ocean reservoir ages. This technique requires sediment cores with sedimentation rates exceeding  $6$ – $10$   $\text{cm ky}^{-1}$ .

Comparison of the  $^{14}\text{C}$  concentration measured for any sample with that calculated for Modern Carbon (MC) after decay over the independently determined age of the sample provides its original  $^{14}\text{C}$  concentration, usually expressed in ‰ deviation from that of the modern standard. To translate ‰  $\Delta^{14}\text{C}$  values for intra-LGM, intra-HS-1, and intra-B/A into apparent age differences between atmosphere and deep-water (= benthic ventilation ages; yr) and to compare these with related DIC, alkalinity, oxygen, and  $\text{PO}_4$  estimates (Table 1; Figs. 2, 4, and 6), we use the  $^{14}\text{C}$  concentrations of the atmosphere and deep ocean during that time, both expressed in MC fraction.

The five techniques all produce  $^{14}\text{C}$  ventilation ages that differ significantly from estimates derived by a simple addition of benthic-planktic age differences to planktic  $^{14}\text{C}$  reservoir ages that are presumed to be constant, or, to deviate only little from a modern average of  $400$ – $550$  yr (Stuiver and Braziunas, 1993), an assumption today indefensible (Reimer et al., 2009). In most cases, the latter estimates will result in deep-water ventilation ages that are by far too low and, in turn, provide calendar age estimates possibly exceeding the actual age by up to  $2000$  yr. Thus we exclude such ages from the data set of this study. For example, this bias applies to various deglacial age estimates published for waters in the North Pacific (e.g., Jaccard et al., 2009; Okazaki et al., 2010) and the upwelling region off Chile (De Polz et al., 2010). Here constant planktic reservoir ages were assumed, which contrasts sharply with short-term shifts

in Holocene reservoir ages that almost reach 900 yr, as reported from the nearby upwelling region off Peru (Fontugne et al., 2004). Various lines of evidence in support of the high planktic reservoir ages that emerge from dating techniques 1–5 are summarized in the Supplement Sect. 1.

In our study, the distribution patterns of ventilation ages are displayed for three glacial-to-deglacial time slices, the  $^{14}\text{C}$  records of which rely on 10 to 12 core sites each (Table 1). Most of them occupy key locations in the ocean MOC, important for tracing the major deep-water masses. The age definitions follow Mix et al. (2001) for the LGM time slice, Denton et al. (2006) and Sarnthein (2011) for HS-1, and the GICC05 age scale (Svensson et al., 2006) for the Bølling (14.7–14.0 ka).

## 4 Deep-water ventilation ages and carbon absorption during LGM and deglacial times

### 4.1 Deep-water ventilation ages and glacial-to-deglacial changes in MOC

We compiled about a dozen fairly robust records of  $^{14}\text{C}$  paleoventilation ages to generate three time slices that tentatively delineate paleocirculation patterns of deep waters for the peak glacial and two deglacial scenarios (Table 1; Fig. 3). Age records from intermediate waters at less than 1500 m were ignored, because intermediate-water circulation tends to follow more small-scale thus complex spatial variations.

Though fragmentary, the data sets listed in Table 1 at least are representative of three key regions for global MOC in the abyssal ocean, namely the North Atlantic onset and the North Pacific terminal region of the modern salinity conveyor belt, and the Atlantic sector of the Southern Ocean. Thus, the paleoreservoir age records do provide a sound first basis for large-scale interpolations, in particular, since LGM and B/A ages of deep waters display a remarkable regional and global homogeneity, except for the North Atlantic (because of longitudinal variations). By contrast, the distribution of HS-1

CPD

9, 925–965, 2013

## $^{14}\text{C}$ reservoir ages and oceanic carbon storage

M. Sarnthein et al.

Title Page

Abstract

Introduction

Conclusions

References

Tables

Figures

⏪

⏩

◀

▶

Back

Close

Full Screen / Esc

Printer-friendly Version

Interactive Discussion



ages does not display a homogenous pattern, the main reason, why we do not assess a global average age for this time slice.

The global trends in the distribution of deep-water  $^{14}\text{C}$  ages reflect an LGM circulation geometry basically similar to today, as far as the prime sources and terminal regions of deep waters in the ocean are concerned. Also, we do not find evidence that the LGM deep-ocean circulation pattern was essentially different. An exception is the Nordic Sea Overflow, the direction of which started to switch between modern and reversed HS-1-style orientation on millennial scales after 21 ka (Sarnthein et al., 2007, plus unpublished data supplemented). Moreover, the relative densities, hence vertical position and flow strength of LGM deep waters differed significantly from today. In the Atlantic, these conclusions obtain independent support from  $\delta^{13}\text{C}$ -based 3-D reconstructions of water mass-specific nutrient contents below 1500 m w.d. (Sarnthein et al., 1994; Curry and Oppo, 2005). Similar  $\delta^{13}\text{C}$  evidence applies to the southwest Pacific, where most records of silt modal grain size suggest a LGM flow strength of deep waters similar to today (McCave et al., 2008).

Most striking – and in contrast to previous conjectures (Broecker et al., 2007) and model predictions (Campin et al., 1999) – is the widespread maximum of LGM ventilation ages in the abyssal Southern Ocean and North Pacific, with values that exceed the modern reference level by 1100–1500 yr and up to 2500 yr (Fig. 3a vs. numerical ranges in Fig. 1; Table 1, and Supplement Sect. 2). Most benthic age estimates were derived by accepting a highly variable  $^{14}\text{C}$  reservoir age of surface waters, at several sites reaching up to 2500 yr. The high planktic age level likewise arises from a direct tuning of  $^{14}\text{C}$  ages to Greenland and Antarctic ice core chronologies (Thornalley et al., 2011; Skinner et al., 2010), from tephrochronology (Waelbroeck et al., 2001; E. Sikes, personal communication, 2012), and from the  $^{14}\text{C}$  plateau technique (Sarnthein et al., 2007). This result is challenging a common, but little substantiated dogma: that past surface waters had largely constant ventilation ages of  $\sim 400$ –500 yr, an alleged modern average (Stuiver and Braziunas, 1993).

**$^{14}\text{C}$  reservoir ages and oceanic carbon storage**

M. Sarnthein et al.

Title Page

Abstract

Introduction

Conclusions

References

Tables

Figures



Back

Close

Full Screen / Esc

Printer-friendly Version

Interactive Discussion



## <sup>14</sup>C reservoir ages and oceanic carbon storage

M. Sarnthein et al.

Title Page

Abstract

Introduction

Conclusions

References

Tables

Figures



Back

Close

Full Screen / Esc

Printer-friendly Version

Interactive Discussion



During HS-1 the spatial distribution of ventilation ages was more complex (Fig. 3b) and clearly contrasted with both the LGM and modern patterns. On the one hand, upper deep waters that stemmed from LGM deep waters in the Southern Ocean, here already starting with ventilation ages of 2000–4000 yr, finally reached extreme, but highly variable ages of > 5000 yr in the “dead-end road” of the northeastern North Atlantic, ages that were totally unexpected prior to Thornalley et al. (2011). These old waters did not originate from southern-source intermediate waters (Burke and Robinson, 2012), but were overlain by somewhat younger intermediate waters found directly to the south and north of Iceland (Thornalley et al., 2011; Sarnthein et al., 2007; Fig. 3b). Obviously the stratification was linked to the salient meltwater stratification caused by the Heinrich-1 iceberg armadas (Sarnthein et al., 2001, and references cited therein). Like the records from the northeastern North Atlantic (Thornalley et al., 2011), the <sup>14</sup>C ventilation ages from the Icelandic Sea (PS2644) suggest that the deepwater circulation system was subject to basic oscillations, with 1000-yr pulses of rejuvenation.

On the other hand, North Pacific deep-water ages then shortly dropped to 1600 yr, thus reflected a transient phase of major age reduction and subpolar deep-water convection down to 3600 m w.d. (Gebhardt et al., 2008), in total perhaps suggesting a short-lasting basic change of the global conveyor belt. Likewise, deep-water ages strongly dropped in the Southern Ocean, so far documented in the Atlantic and West Australian sectors (Skinner et al., 2010; Sarnthein et al., 2011). Altogether, the abyssal ocean probably experienced a major net rejuvenation during HS-1.

In contrast to HS-1, low ventilation ages during the Bølling suggest that the North Atlantic MOC had already returned to the modern mode (Fig. 3c). However, different from today, low ventilation ages of 1500 yr and less continued in the northern North Pacific from HS-1 over the Bølling and reflected ongoing deep-water convection. Hence, the deglacial reversals in overturning circulation were not necessarily coupled at the Pacific and North Atlantic ends of the “global conveyor belt”, a pattern still difficult to value on the basis of our limited number of ventilation age records.

## 4.2 LGM absorption of carbon in the deep ocean

Extrapolating the regression displayed in Fig. 2a, b, we now can roughly constrain the amounts of total carbon additionally stored in the LGM deep ocean. Modern  $^{14}\text{C}$  ages spread almost uniformly between  $\sim 600$  and  $2400$  yr. The average apparent ventilation age of  $\sim 1500$  yr is equal to a  $^{14}\text{C}$  value of  $-170\%$ . In turn, the peak glacial arithmetic mean derives from benthic ventilation ages ranging between  $600$  and  $\sim 3600$  yr in the open ocean (excluding the segregated South China Sea; Fig. 3c), hence amounts to  $2100$  yr ( $-230\%$   $^{14}\text{C}$ ; calculated for “paleo”-Modern Carbon =  $1.0$ ),  $600$  yr more than today. This average reveals an LGM deep ocean that was able to absorb and store a huge amount of additional carbon transferred from the atmosphere and terrestrial biosphere (Fig. 2b).

This conclusion is not hampered by a potential LGM rise in the flow rate of Antarctic Bottom Water (AABW) as suggested by Campin et al. (1999). An increase of this flow rate would not affect our extrapolation of the DIC–age relationship to the past, because the relationship of modern AABW does not deviate noticeably from that of NADW, as shown in Fig. 2a. Moreover, all  $^{14}\text{C}$  ventilation ages so far published (Table 1 and Sikes et al., 2011), likewise benthic  $\delta^{13}\text{C}$  transects off New Zealand (McCave et al., 2008), do not suggest an enhanced, but a strongly reduced LGM downwelling of rejuvenated AABW.

Viceversa, a breakdown of glacial stratification of subpolar surface waters during HS-1 induced a massive and almost abrupt rejuvenation of deep waters in two key regions of the ocean. On the basis of a transient sudden  $\sim 200\%$  drop in the benthic-planktic  $^{14}\text{C}$  offset (Gebhardt et al., 2008; now corroborated by further unpubl. benthic  $^{14}\text{C}$  ages), vigorous deep-mixing and deep-water formation reached in the northern North Pacific down to  $> 3600$  m w.d. from  $17.4$ – $16.0$  ka (Fig. 3), which implies a major carbon release. This evidence is opposed to Jaccard and Galbraith (2012) who postulate a sustained stratification until the B/A, a claim unsupported by adequately dated and resolved millennial-to-centennial-scale proxy records. – Likewise, the Southern Ocean

### $^{14}\text{C}$ reservoir ages and oceanic carbon storage

M. Sarnthein et al.

Title Page

Abstract

Introduction

Conclusions

References

Tables

Figures



Back

Close

Full Screen / Esc

Printer-friendly Version

Interactive Discussion



(Skinner et al., 2010) reflects a phase of enhanced vertical mixing during HS-1 and in turn, a significant deglacial transfer of carbon back to the atmosphere and terrestrial biosphere (Crowley, 2011).

Extrapolating the regression lines displayed in Fig. 2b we roughly constrain the amounts of total carbon additionally stored in the LGM deep ocean. The modern average  $^{14}\text{C}$  value of  $-170\text{‰}$  corresponds to a global average of  $2265\ \mu\text{mol DIC kg}^{-1}\ \text{H}_2\text{O}$  dissolved in the modern deep ocean. By comparison, the LGM  $^{14}\text{C}$  value of  $-230\text{‰}$  reflects an average DIC of  $2350\text{--}2380\ \mu\text{mol kg}^{-1}\ \text{H}_2\text{O}$ ,  $85\text{--}115\ \mu\text{mol}$  higher than today, a range reflecting the different slope gradients of regression lines for regions 1, 2, 4, and 6 and ignoring regions 3 and 5 (Fig. 5). These LGM estimates are based on the assumption that the modern variability range of marine biological production overall remained widely constant from interglacial to glacial times (Sigman and Boyle, 2000), thus resulted in a largely constant global flux of organic and inorganic particulate carbon, summing up to an average of  $1.1\ \text{Gt yr}^{-1}$ .

Likewise, the impact of the “solubility pump plus preformed carbon” turned out almost constant during the LGM, mainly because of the opposed effects of reduced SST and increased SSS in downwelling regions versus that of decreased atmospheric  $p\text{CO}_2$ . Here we assume that upwelling, renewed aeration, and  $^{14}\text{C}$  enrichment of NADW in the Weddell Sea ceased during the LGM as a result of enlarged perennial sea ice (Gersonde et al., 2003; Sigman et al., 2010). Our conclusion is fully supported by McCave et al. (2008), who depict a benthic  $\delta^{13}\text{C}$  transect from the Southwest Pacific at  $2000\text{--}3500\ \text{m w.d.}$ , where  $\delta^{13}\text{C}$  dropped by  $1.0\text{--}1.3\text{‰}$  from Holocene to LGM times at  $2000\text{--}3400\ \text{m depth}$ , but likewise at  $3500\text{--}4800\ \text{m w.d.}$ , that is in the range of Lower Circumpolar Deepwater.

In total, the LGM rise in DIC may correspond – disregarding the modern DIC-age relationship for the southern South Pacific – to  $\sim 730\text{--}980\ \text{Gt}$  additional carbon stored in the global deep ocean below  $2000\ \text{m w.d.}$  This amount clearly exceeds the estimate of  $\sim 530\ \text{Gt}$  carbon, that sums up the Late-Holocene-to-glacial transfer of atmospheric  $200\ \text{Gt}$  carbon plus  $\sim 330\ \text{Gt}$  carbon derived from the terrestrial biosphere and soils

## $^{14}\text{C}$ reservoir ages and oceanic carbon storage

M. Sarnthein et al.

Title Page

Abstract

Introduction

Conclusions

References

Tables

Figures



Back

Close

Full Screen / Esc

Printer-friendly Version

Interactive Discussion



(Monnin et al., 2001; Ciais et al., 2012). To accommodate a total of 530 Gt carbon in the LGM abyssal ocean would require a rise in average deep-water age by no more than 325–440 yr.

In addition to the carbon transfer from atmosphere and biosphere, the average aging by 600 yr reflects an LGM drawdown of 200–450 Gt carbon into the abyssal ocean (Fig. 2b). The latter carbon mass may have been derived from the significant carbon release from glacial Atlantic and Pacific intermediate waters, that is suggested by benthic  $\Delta^{13}\text{C}$  and  $^{14}\text{C}$  transects (Duplessy et al., 1989; Sarnthein et al., 1994; Curry and Oppo, 2005). However, the number of robust  $^{14}\text{C}$  ventilation ages from intermediate waters at less than 1500–2000 m (Bryan et al., 2010; Sarnthein, 2011; Robinson et al., 2005; Rose et al., 2010; Burke and Robinson, 2012) is still too low and spotty in the three oceans for developing a sound estimate of the LGM carbon storage in this complex layer of intermediate waters (Hain et al., 2010).

### 4.3 Implications for LGM oxygen contents, alkalinity, and $\text{CaCO}_3$ dissolution

The significantly increased residence times of ocean deep waters imply a considerable local drop in glacial deep-water  $\text{O}_2$  (Fig. 6). Assuming a general rise in  $\text{O}_2$  solubility during the LGM (+20  $\mu\text{mol O}_2$ ; based on the same assumptions as outlined for the DIC transfer function), data listed in Table 1 show that the LGM deep Southern Ocean and the North Pacific basins may indeed have reached a suboxic  $\text{O}_2$  level in bottom waters, assuming  $\sim 10 \mu\text{mol O}_2 \text{ kg}^{-1}$  as crucial boundary (Stramma et al., 2008). These estimates provide support for Boyle's (1988a, b) "nutrient deepening hypothesis" that implies a vertical shift of oxygen depletion from intermediate to deep-ocean waters. By and large, our estimates also agree with the patterns of Jaccard and Galbraith (2012). By contrast, during HS-1  $\text{O}_2$  dropped to zero in the northeast Atlantic only, a value effectively documented by rudimentary laminations in sediments at  $\sim 3060$  m w.d. south of the Azores (core MD08-3180; H. Kinkel, personal communication, 2012).

Our  $^{14}\text{C}$ -based conclusions on glacial-to-deglacial changes in the carbon sequestration of the deep ocean agree with various findings, trends, and concepts recently

CPD

9, 925–965, 2013

## $^{14}\text{C}$ reservoir ages and oceanic carbon storage

M. Sarnthein et al.

Title Page

Abstract

Introduction

Conclusions

References

Tables

Figures

◀

▶

◀

▶

Back

Close

Full Screen / Esc

Printer-friendly Version

Interactive Discussion



published on the basis of model simulations (Huiskamp and Meissner, 2012), marine-based  $^{14}\text{C}$  records, and various other proxies. For example, combined evidence of benthic foraminiferal  $\Delta^{14}\text{C}$  and boron/calcium ratios (Yu et al., 2010) suggests that > 100 GtC were released from the deglacial deep ocean to the atmosphere during early deglacial times.

A significantly prolonged residence time of deep waters may have strengthened  $\text{CaCO}_3$  dissolution during the LGM (Archer et al., 2004), thus supplying additional dissolved carbon and alkalinity to the abyssal ocean. An enhanced supply is reflected by the slope of POTALK vs.  $^{14}\text{C}$ , which amounts to  $1 \mu\text{mol kg}^{-1}/\text{‰}^{14}\text{C}$  as compared to the slope of DIC, that is  $1.22 \mu\text{mol kg}^{-1}/\text{‰}^{14}\text{C}$ . Since absolute POTALK values are higher than DIC and the gradient of the age–DIC slope is steeper than that of age–POTALK (Figs. 2a vs. 4), the difference between POTALK and DIC, which approximates the carbonate ion concentration, will progressively decrease with rising  $^{14}\text{C}$  reservoir ages. Accordingly, the increasingly lowered difference between increased alkalinity (Fig. 4) and DIC (Fig. 2b) will lead to a major drop in deep-ocean carbonate ion concentrations ( $\text{CO}_3^{2-}$ ) (Table 1) and thus, to a significant rise of glacial  $\text{CaCO}_3$  dissolution in several ocean basins.

Peak glacial  $\text{CO}_3^{2-}$  concentrations decreased by  $\sim 65$  to  $> 120 \mu\text{mol kg}^{-1}$  in the Atlantic, western Southern Ocean, and Pacific, however, by no more than  $\sim 0$ – $65 \mu\text{mol kg}^{-1}$  in the eastern Indian Ocean and western North Atlantic, where dissolution did hardly increase (Yu et al., 2010). Indeed, well dated and highly resolved sediment records clearly suggest poor  $\text{CaCO}_3$  preservation in both the deep north-western and northeastern North Pacific (Gebhardt et al., 2008). These results contrast with the traditional view asserting a peak glacial maximum in Pacific  $\text{CaCO}_3$  preservation. Possibly, the carbonate spikes widely reported from the LGM Equatorial Pacific do actually belong to HS-1 and B/A (e.g., as properly classified by Anderson et al., 2008) in regions, where (1) sedimentation rates hardly exceed  $1.0$ – $1.5 \text{ cm ky}^{-1}$ , (2) past variations in planktic  $^{14}\text{C}$  reservoir age are largely unknown, (3) benthic  $\delta^{18}\text{O}$  records may lag the atmospheric records of climate change by up to  $> 2000 \text{ yr}$  (Duplessy et al.,

CPD

9, 925–965, 2013

## $^{14}\text{C}$ reservoir ages and oceanic carbon storage

M. Sarnthein et al.

Title Page

Abstract

Introduction

Conclusions

References

Tables

Figures

◀

▶

◀

▶

Back

Close

Full Screen / Esc

Printer-friendly Version

Interactive Discussion



1991b; Gebhardt et al., 2008), and (4) orbital age control is insufficient to resolve the age difference between the two intervals.

#### 4.4 Outlook on changing carbonate dissolution over HS-1 and B/A – implications for changes in atmospheric $^{14}\text{C}$

5 During HS-1 the abyssal ocean on the whole probably experienced a net rejuvenation (Fig. 3b) with the deglacial breakdown of bipolar surface water stratification (Gebhardt et al., 2008, as outlined above), accompanied by a major bipolar release of carbon dioxide. Nevertheless, our data resolution does not yet allow a rudimentary quantification of the overall MOC patterns, because they were more complex than during the LGM. A significant rise in  $\text{CO}_3^{2-}$  concentrations in the eastern Indian and North Pacific oceans ( $\sim 5\text{--}46\ \mu\text{mol kg}^{-1}$ ; Table 1) suggests a preservation spike of deep-water carbonate, which indeed is recorded in late-HS-1 sediment sections (Gebhardt et al., 2008), in particular from the South China Sea (Miao and Thunnell, 1994), coeval with maximum dissolution in the northeast Atlantic.

15 During the B/A (Fig. 3c) hardly any  $^{14}\text{C}$  ventilation age of the abyssal ocean exceeds 2000 yr (Table 1). On the basis of Fig. 2, this significant general rejuvenation suggests a major drop in the carbon inventory of the deep ocean down to the modern level as early as during (late) HS-1. Our estimates exceed significantly the pre-Bølling carbon transfer inferred from the ice core record of atmospheric  $\text{CO}_2$  ( $\Delta 100\ \text{Gt C}$ ; Monnin et al., 2001), hence may explain both a fast growing biosphere uptake near the end of this interval and most important, the 190-‰ decrease in atmospheric  $\Delta^{14}\text{C}$  over this interval (Ramsey et al., 2012). In contrast to Broecker and Barker (2007) we regard this  $\Delta^{14}\text{C}$  drop as well consistent with the deglacial changes in carbon and  $^{14}\text{C}$  contents we outlined for deepwater paleoceanography.

25 To arrive at this conclusion, we assume for simplicity (1) that atmospheric  $^{14}\text{C}$  production remained constant over HS-1 (Skinner et al., 2010). (2) We calculate the effect of a transfer of the  $^{14}\text{C}$  depleted excess carbon (730–980 Gt DIC) from the LGM deep

CPD

9, 925–965, 2013

### $^{14}\text{C}$ reservoir ages and oceanic carbon storage

M. Sarnthein et al.

Title Page

Abstract

Introduction

Conclusions

References

Tables

Figures



Back

Close

Full Screen / Esc

Printer-friendly Version

Interactive Discussion



ocean to the LGM atmosphere during HS-1. (3) We consider that the LGM atmosphere contained 190 ppm CO<sub>2</sub> (~375 GtC) with a <sup>14</sup>C concentration 1.4 times higher than that of the standard modern atmosphere (fMC) (Ramsey et al., 2012). The average reservoir age of the LGM deep ocean of 2100 yr means that its <sup>14</sup>C concentration was 0.77 times that of the LGM atmosphere, 1.08 times that of the modern atmosphere (fMC).

Direct admixture of the excess abyssal carbon to the LGM atmosphere gives the following result: 375 GtC · 1.4 fMC + 730/980 GtC · 1.08 fMC add up to a mixture of 1105/1355 GtC with a <sup>14</sup>C concentration of 1.19–1.17 fMC, which implies a deglacial 210–230-‰ drop in atmospheric fMC.

These values directly compare with 1.2 fMC recorded for the atmosphere during the early B/A (Ramsey et al., 2012) and indicate that the early B/A atmospheric <sup>14</sup>C and hence, the early deglacial 190-‰ drop in atmospheric <sup>14</sup>C can indeed be reproduced by the admixture of <sup>14</sup>C-depleted carbon from the LGM deep ocean, a shift that previously was claimed to be not explicable, a “mystery”.

In reality, of course, the early B/A atmosphere contained only 240 ppm CO<sub>2</sub> (~475 GtC), which means that more than 85 % (i.e. 630/880 out of 730/980 Gt) of the <sup>14</sup>C-depleted carbon released from the deep ocean were admixed from the atmosphere back into intermediate and surface waters of the ocean, over HS-1 also to the deep North Atlantic (Fig. 3), and a minor part to the terrestrial biosphere near the onset of B/A. A thorough general-circulation model study will be needed to predict in detail the deglacial redistribution patterns of the immense <sup>14</sup>C-depleted carbon masses from the deep ocean pool up to the various carbon inventories of the ocean, bio- and atmosphere. Also, we will need to constrain more closely the differential capacity of the key regions in the deglacial deep ocean to sequester or release carbon from or into the terrestrial biosphere and atmosphere, in particular to establish a much denser network of 3-D paleoventilation-age transects both in the subpolar North Pacific and in the Southern Ocean.

## <sup>14</sup>C reservoir ages and oceanic carbon storage

M. Sarnthein et al.

Title Page

Abstract

Introduction

Conclusions

References

Tables

Figures

⏪

⏩

◀

▶

Back

Close

Full Screen / Esc

Printer-friendly Version

Interactive Discussion



In summary, we conclude that over HS-1 the upper deep waters of the abyssal ocean were subject to a distinct outgassing and early deglacial rejuvenation by an average of 600  $^{14}\text{C}$  yr and more. This was fully sufficient to account for a 190-permil drop in atmospheric  $^{14}\text{C}$  over HS-1, which is also reflected by two major atmospheric  $^{14}\text{C}$  plateaus (Sarnthein et al., 2007).

## 5 Conclusions

Using the modern global distributions of apparent  $^{14}\text{C}$  ventilation ages and DIC we established a new transfer function to reconstruct past changes in the carbon storage of ocean deep waters. On this basis we concluded tentatively on a potential rise of the LGM carbon inventory by approximately 730–980 Gt vs. pre-industrial times. This amount compares well with an estimated glacial transfer of 530–700 Gt from both the atmosphere and terrestrial biosphere in addition to a major DIC relocation from ocean intermediate waters. During the early deglacial HS-1, a large portion of this  $^{14}\text{C}$  depleted carbon was released to the atmosphere and terrestrial biosphere. Accordingly, an alleged major “mystery” of last deglacial times, the source of  $^{14}\text{C}$ -depleted additional atmospheric carbon, appears solved.

The peak glacial deep ocean is emerging as “cold acidic ocean”, regionally with low  $\text{O}_2$  concentrations, because of the prolonged residence time of deep waters, in harmony with the decreased LGM difference between potential alkalinity and DIC, in particular in the Atlantic and Pacific. This finding matches the glacial maximum in  $\text{CaCO}_3$  dissolution for Atlantic sediments, particularly during HS-1, known since the first days of paleoceanography (Olausson, 1965; Berger, 1973).

**Supplementary material related to this article is available online at:**  
<http://www.clim-past-discuss.net/9/925/2013/cpd-9-925-2013-supplement.pdf>.

*Acknowledgements.* We acknowledge fruitful discussions with Andreas Oschlies, Kiel, and Michael Schulz and André Paul, Bremen, careful and constructive anonymous reviews of an early manuscript version, and valuable suggestions of Jean-Claude Duplessy, Gif-sur-Yvette. Moreover, we thank the Leibniz Laboratory, University of Kiel, for hundreds of careful radio-carbon analyses made over the years. MS and PMG were supported by funds of DFG grant Sa207/48-1. BS acknowledges funding from the Cluster of Excellence the Future Ocean (EXC-80/1), the Collaborative Research Centre SFB 754 by the German Science Foundation (DFG), and from BIOACID by the German Ministry of Education and Research (BMBF 03F0608M).

## References

- Adkins, J. F., Cheng, H., Boyle, E. A., Druffel, E. R. M., and Edwards, R. L.: Deep-sea coral evidence for rapid change in ventilation of the deep North Atlantic 15,400 yr ago, *Science*, 280, 725–728, 1998.
- Amante, C. and Eakins, B. W.: ETOPO1 1 Arc-Minute Global Relief Model: Procedures, Data Sources and Analysis, NOAA Techn. Memorandum NESDIS, NGDC-24, 19 pp., 2009.
- Anderson, R. F., Fleisher, M. Q., Lao, Y., and Winckler, G.: Modern CaCO<sub>3</sub> preservation in equatorial Pacific sediments in the context of Late-Pleistocene glacial cycles, *Mar. Chem.*, 111, 30–46, 2008.
- Antia, A. N., Koeve, W., Fischer, G., Blanz, T., Schulz-Bull, D., Scholten, J., Neuer, S., Kremling, K., Kuss, J., Peinert, R., Hebbeln, D., Bathmann, U., Conte, M., Fehner, U., and Zeitzschel, B.: Basin-wide particulate carbon flux in the Atlantic Ocean: regional export patterns and potential for atmospheric CO<sub>2</sub> sequestration, *Global Biogeochem. Cy.*, 15, 845–862, 2001.
- Archer, D. and Winguth, A.: What caused the glacial/interglacial atmospheric pCO<sub>2</sub> cycles?, *Rev. Geophys.*, 38, 159–189, 2000.
- Archer, D., Martin, P., Buffett, B., Brovkin, V., Rahmstorf, S., and Ganopolski, A.: The importance of ocean temperature to global biogeochemistry, *Earth Planet. Sc. Lett.*, 222, 333–348, 2004.
- Bard, E.: Geochemical and geophysical implications of the radiocarbon calibration, *Geochim. Cosmochim. Ac.*, 62, 2025–2038, 1998.

## <sup>14</sup>C reservoir ages and oceanic carbon storage

M. Sarnthein et al.

Title Page

Abstract

Introduction

Conclusions

References

Tables

Figures



Back

Close

Full Screen / Esc

Printer-friendly Version

Interactive Discussion



- Barker, S., Knorr, G., Vautravers, M. J., Diz, P., and Skinner, L. C.: Extreme deepening of the Atlantic overturning circulation during deglaciation, *Nat. Geosci.*, 3, 567–571, doi:10.1038/NGEO921, 2010.
- Basak, C., Martin, E. E., Horikawa, K., and Marchitto, T. M.: Southern Ocean source of <sup>14</sup>C-depleted carbon in north Pacific Ocean during the last deglaciation, *Nat. Geosci.*, 3, 770–774, 2010.
- Berger, W. H.: Deep-sea carbonates. Pleistocene dissolution cycles, *J. Foramin. Res.*, 3, 187–193, 1973.
- Berger, W. H. and Keir, R. S.: Glacial-Holocene changes in atmospheric CO<sub>2</sub> and the deep-sea record, *AGU Geophys. Monogr.*, 29, 337–351, 1984.
- Boyle, E. A.: The role of vertical chemical fractionation in controlling late Quaternary atmospheric carbon-dioxide, *J. Geophys. Res.-Ocean*, 93, 15701–15714, 1988a.
- Boyle, E. A.: Vertical oceanic nutrient fractionation and glacial interglacial CO<sub>2</sub> cycles, *Nature*, 331, 55–56, 1988b.
- Broecker, W. S.: Glacial-to-interglacial changes in ocean chemistry, *Prog. Oceanogr.*, 11, 151–197, 1982.
- Broecker, W. S.: The great ocean conveyor, *Oceanography*, 4, 79–89, 1991.
- Broecker, W. and Barker, S. A.: 190‰ drop in atmosphere's Δ<sup>14</sup>C during the “Mystery Interval”, *Earth Planet. Sc. Lett.*, 256, 90–99, 2007.
- Broecker, W., Barker, S., Clark, E., Hajdas, I., Bonani, G., and Stott, L.: Ventilation of the Glacial deep Pacific Ocean, *Science*, 306, 1169–1172, 2004.
- Broecker, W., Clark, E., Barker, S., Hajdas, I., Bonani, G., and Moreno, E.: Radiocarbon age of late glacial deep waters from the equatorial Pacific, *Paleoceanography*, 22, PA2206, doi:10.1029/2006PA001359, 2007.
- Bryan, S. P., Marchitto, T. M., and Lehman, S. J.: The release of <sup>14</sup>C-depleted carbon from the deep ocean during the last deglaciation: evidence from the Arabian Sea, *Earth Planet. Sc. Lett.*, 298, 244–254, 2010.
- Burke, A. and Robinson, L. F.: The Southern Ocean's role in carbon exchange during the last deglaciation, *Science*, 335, 557–561, 2012.
- Ciais, P., Tagliabue, A., Cuntz, M., Bopp, L., Scholze, M., Hoffmann, G., Louranton, A., Harrison, S. P., Prentice, I. C., Kelley, D. I., Koven, C., and Piao, S. L.: Large inert carbon pool in the terrestrial biosphere during the Last Glacial Maximum, *Nat. Geosci.*, 5, 74–79, 2012.

## <sup>14</sup>C reservoir ages and oceanic carbon storage

M. Sarnthein et al.

[Title Page](#)

[Abstract](#)

[Introduction](#)

[Conclusions](#)

[References](#)

[Tables](#)

[Figures](#)



[Back](#)

[Close](#)

[Full Screen / Esc](#)

[Printer-friendly Version](#)

[Interactive Discussion](#)



- Crowley, T. J.: Proximal trigger for late glacial Antarctic circulation and CO<sub>2</sub> changes, *PAGES News*, 19, 70–71, 2011.
- Campin, J.-M., Fichefet, T., and Duplessy, J.-C.: Problems with using radiocarbon to infer ocean ventilation rates for past and present climates, *Earth Planet. Sc. Lett.*, 165, 17–24, 1999.
- Curry, W. B. and Oppo, D. W.: Glacial water mass geometry and the distribution of  $\delta^{13}\text{C}$  of  $\Sigma\text{CO}_2$  in the western Atlantic Ocean, *Paleoceanography*, 20, PA1017, doi:10.1029/2004PA001021, 2005.
- Denton, G. H., Broecker, W. S., and Alley, R. B.: The Mystery Interval 17.5–14.5 kyr ago, *PAGES News*, 14, 14–16, 2006.
- De Pol-Holz, R., Keigwin, L., Southon, J., Hebbeln, D., and Mohtadi, M.: No signature of abyssal carbon in intermediate waters off Chile during deglaciation, *Nat. Geosci.*, 3, 192–195, 2010.
- Duplessy, J.-C., Arnold, M., Bard, E., Juillet-Leclerc, A., Kallel, N., and Labeyrie, L.: AMS <sup>14</sup>C study of transient events and of the ventilation rate of the Pacific intermediate water during the last deglaciation, *Radiocarbon*, 31, 493–502, 1989.
- Duplessy, J. C., Labeyrie, L., Juillet-Leclerc, A., Maitre, F., Duprat, J., and Sarnthein, M.: Surface salinity reconstruction of the North Atlantic Ocean during the Last Glacial Maximum, *Oceanol. Acta*, 14, 311–324, 1991a.
- Duplessy, J.-C., Bard, E., Arnold, M., Shackleton, N. J., Duprat, J., and Labeyrie, L. D.: How fast did the ocean-atmosphere system run during the last deglaciation?, *Earth Planet. Sc. Lett.*, 103, 27–40, 1991b.
- Fontugne, M., Carré, M., Bentaleb, I., Julien, M., and Lavallée, D.: Radiocarbon reservoir age variations in the South Peruvian upwelling during the Holocene, *Radiocarbon*, 46, 531–537, 2004.
- Franke, J., Schulz, M., Paul, A., and Adkins, A. F.: Assessing the ability of the <sup>14</sup>C projection-age method to constrain the circulation of the past in a 3-D ocean model, *Geochem. Geophys. Geosy.*, 9, Q08003, doi:10.1029/2008GC001943, 2008.
- Gebhardt, H., Sarnthein, M., Kiefer, T., Erlenkeuser, H., Schmieder, F., and Röhl, U.: Paleonutrient and paleoproductivity records from the subarctic North Pacific for Pleistocene glacial terminations I to V, *Paleoceanography*, 23, PA4212, doi:10.1029/2007PA001513, 2008.
- Gersonde, R., Abelmann, A., Brathauer, U., Becquey, S., Bianchi, C., Cortese, G., Grobe, H., Kuhn, G., Niebler, H.-S., Segl, M., Sieger, R., Zielinski, U., and Fütterer, D. K.: Last glacial

## <sup>14</sup>C reservoir ages and oceanic carbon storage

M. Sarnthein et al.

[Title Page](#)

[Abstract](#)

[Introduction](#)

[Conclusions](#)

[References](#)

[Tables](#)

[Figures](#)



[Back](#)

[Close](#)

[Full Screen / Esc](#)

[Printer-friendly Version](#)

[Interactive Discussion](#)



sea surface temperatures and sea-ice extent in the Southern Ocean (Atlantic-Indian sector): a multiproxy approach, *Paleoceanography*, 18, 1061, doi:10.1029/2002PA000809, 2003.

Hain, M. P., Sigman, D. M., and Haug, G. H.: Shortcomings of the isolated abyssal reservoir model for deglacial radiocarbon changes in the mid-depth Indo-Pacific Ocean, *Geophys. Res. Lett.*, 38, L04604, doi:10.1029/2010GL046158, 2011.

Huiskamp, W. N. and Meissner, K. J.: Oceanic carbon and water masses during the Mystery Interval: a model-data comparison study, *Paleoceanography*, 27, PA4206, 1–17, doi:10.1029/2012PA002368, 2012.

Jaccard, S. L. and Galbraith, E. D.: Large climate-driven changes of oceanic oxygen concentrations during the last deglaciation, *Nat. Geosci.*, 5, 151–156, doi:10.1038/ngeo1352, 2012.

Jaccard, S. L., Galbraith, E. D., Sigman, D. M., Haug, G. H., Francois, R., Pedersen, T. F., Dulski, P., and Thierstein, H. R.: Subarctic Pacific evidence for a glacial deepening of the oceanic respired carbon pool, *Earth Planet. Sc. Lett.*, 277, 156–165, 2009.

Key, R. M., Kozyr, A., Sabine, C. L., Lee, K., Wanninkhof, R., Bullister, J. L., Feely, R. A., Millero, F. J., Mordy, C., and Peng, T.-H.: A global ocean carbon climatology: results from Global Data Analysis Project (GLODAP), *Global Biogeochem. Cy.*, 18, GB4031, doi:10.1029/2004GB002247, 2004.

Köhler, P., Fischer, H., Munhoven, G., and Zeebe, R. E.: Quantitative interpretation of atmospheric carbon records over the last glacial termination, *Global Biogeochem. Cy.*, 19, GB4020, doi:10.1029/2004GB002345, 2005.

McCave, I. N., Carter, L., and Hall, I. R.: Glacial-interglacial changes in water mass structure and flow in the SW Pacific Ocean, *Quaternary Sci. Rev.*, 27, 1886–1908, 2008.

Marchitto, T., Lehman, S., Ortiz, J., Fluckiger, J., and van Geen, A.: Marine radiocarbon evidence for the mechanism of deglacial atmospheric CO<sub>2</sub> rise, *Science*, 316, 1456–1459, 2007.

Matsumoto, K.: Radiocarbon-based circulation age of the world oceans, *J. Geophys. Res.*, 112, C09004, doi:10.1029/2007JC004095, 2007.

McCave, I. N., Carter, L., and Hall, I. R.: Glacial-interglacial changes in water mass structure and flow in the SW Pacific Ocean, *Quaternary Sci. Rev.*, 27, 1886–1908, 2008.

Miao, Q. and Thunnell, R. C.: Glacial-Hoocene carbonate dissolution and sea surface temperatures in the South China and Sulu seas, *Paleoceanography*, 9, 269–290, 1994.

Mikaloff Fletcher, S. E., Gruber, N., Jacobson, A. R., Doney, S. C., Dutkiewicz, S., Gerber, M., Follows, M., Joos, F., Lindsay, K., Menemenlis, D., Mouchet, A., Müller, S. A., Sarmiento,

## <sup>14</sup>C reservoir ages and oceanic carbon storage

M. Sarnthein et al.

Title Page

Abstract

Introduction

Conclusions

References

Tables

Figures



Back

Close

Full Screen / Esc

Printer-friendly Version

Interactive Discussion



- J. L.: Inverse estimates of anthropogenic CO<sub>2</sub> uptake, transport, and storage by the ocean, *Global Biogeochem. Cy.*, 20, GB2002, doi:10.1029/2005GB002530, 2006.
- Mix, A. C., Bard, E., and Schneider, R.: Environmental processes of the Ice age: land, oceans, glaciers (EPILOG), *Quaternary Sci. Rev.*, 20, 627–658, 2001.
- 5 Monnin, E., Indermühle, A., Dällenbach, A., Flückiger, J., Stauffer, B., Stocker, T. F., Raynaud, D., and Barnola, J.-M.: Atmospheric CO<sub>2</sub> concentrations over the last glacial termination, *Science*, 291, 112–114, 2001.
- Negre, C., Zahn, R., Thomas, A. L., Masque, P., Henderson, G. M., Martínez-Méndez, G., Hall, I. R., and Mas, J. L.: Reversed flow of Atlantic deep water during the Last Glacial Maximum, *Nature*, 468, 84–88, 2010.
- 10 Okazaki, Y., Timmermann, A., Menviel, L., Harada, N., Abe-Ouchi, A., Chikamoto, M. O., Mouchet, A., and Asahi, H.: Deepwater formation in the North Pacific during the last glacial termination, *Science*, 329, 200–204, 2010.
- Olausson, E.: Evidence of climatic changes in North-Atlantic deep-sea cores with remarks on isotopic paleotemperature analysis, *Prog. Oceanogr.*, 3, 221–252, 1965.
- 15 Orsi, A. H., Smethie, W. M., and Bullister, J. L.: On the total input of Antarctic waters to the deep ocean: a preliminary estimate from chlorofluorocarbon measurements, *J. Geophys. Res.-Ocean*, 107, C83122, doi:10.1029/2001JC000976, 2002.
- Pflaumann, U., Sarnthein, M., Chapman, M., Funnell, B., Huels, M., Kiefer, T., Maslin, M., Schulz, H., Swallow, J., van Kreveld, S., Vautravers, M., Vogelsang, E., Weinelt, M.: The glacial North Atlantic: sea surface conditions reconstructed by GLAMAP-2000, *Paleoceanography*, 18, 1–28, doi:10.1029/2002PA000774, 2003.
- 20 Rahmstorf, S.: Thermohaline ocean circulation, in: *Encyclopedia of Quaternary Sciences*, Elsevier, 1–10, 2006.
- 25 Ramsey, C. B., Staff, R. A., Bryant, C. L., Brock, F., Kitagawa, H., van der Plicht, J., Scholaut, G., Marshall, M. H., Brauer, A., Lamb, H. F., Payne, R. L., Tarasov, P. E., Haraguchi, T., Gotanda, K., Yonenobu, H., Yokoyama, Y., Tada, R., and Nakagawa, T.: A complete terrestrial radiocarbon record for 11.2 to 52.8 kyr BP, *Science*, 338, 370–374, 2012.
- Raven, J. A. and Falkowski, P. G.: Oceanic sinks for atmospheric CO<sub>2</sub>, *Plant Cell Environ.*, 22, 741–755, 1999.
- 30 Redfield, A. C., Ketchum, B. H., and Richards, F. A.: The influence of organisms on the composition of sea-water, in: *The Sea*, Vol. 2, edited by: Hill, M. N., John Wiley & Sons, New York, 26–77, 1963.

**<sup>14</sup>C reservoir ages  
and oceanic carbon  
storage**

M. Sarnthein et al.

Title Page

Abstract

Introduction

Conclusions

References

Tables

Figures



Back

Close

Full Screen / Esc

Printer-friendly Version

Interactive Discussion

- Reimer, P. J., Baillie, M. G. L., Bard, E., Bayliss, A., Beck, J. W., Blackwell, P. G., Ramsey, C. B., Buck, C. E., Burr, G. S., Edwards, R. L., Friedrich, M., Grootes, P. M., Guilderson, T. P., Hajdas, I., Heaton, T. J., Hogg, A. G., Hughen, K. A., Kaiser, K. F., Kromer, B., McCormac, F. G., Manning, S. W., Reimer, R. W., Richards, D. A., Southon, J. R., Talamo, S., Turney, C. S. M., van der Plicht, J., and Weyhenmeyer, C. E.: INTCAL09 and MARINE09 radiocarbon age calibration curves, 0–50 000 yr cal BP, *Radiocarbon*, 51, 1111–1150, 2009.
- Robinson, L. R., Adkins, J. F., Keigwin, L. D., Southon, J., Fernandez, D. P., Wang, S.-L., and Scheirer, D. S.: Radiocarbon variability in the western North Atlantic during the last deglaciation, *Science*, 310, 1469–1473, 2005.
- Rose, K. A., Sikes, E. L., Guilderson, T. P., Shane, P., Hill, T. M., Zahn, R., and Spero, H. J.: Upper-ocean-to atmosphere radiocarbon offsets imply fast deglacial carbon dioxide release, *Nature*, 466, 1093–1097, 2010.
- Sarmiento, J. L. and Gruber, N.: *Ocean Biogeochemical Dynamics*, Princeton University Press, Princeton, NJ, 526 pp., 2006.
- Sarnthein, M.: Northern meltwater pulses, CO<sub>2</sub> and Atlantic ocean convection, *Science*, 331, 156–158, 2011.
- Sarnthein, M., Winn, K., Jung, S., Duplessy, J. C., Labeyrie, L., Erlenkeuser, H., and Ganssen, G.: Changes in East Atlantic deepwater circulation over the last 30,000 yr – an eight-time-slice record, *Paleoceanography*, 9, 209–267, 1994.
- Sarnthein, M., Statterger, K., Dreger, D., Erlenkeuser, H., Grootes, P., Haupt, B., Jung, S., Kiefer, T., Kuhnt, W., Pflaumann, U., Schäfer-Neth, C., Schulz, H., Schulz, M., Seidov, D., Simstich, J., van Kreveld-Alfane, S., Vogelsang, E., Völker, A., and Weinelt, M.: Fundamental modes and abrupt changes in North Atlantic circulation and climate over the last 60 kyr – concepts, reconstruction, and numerical modelling, in: *The Northern North Atlantic: A Changing Environment*, edited by: Schäfer, P., Ritzrau, W., Schlüter, M., and Thiede, J., Springer, 365–410, 2001.
- Sarnthein, M., Grootes, P. M., Kennett, J. P., and Nadeau, M.-J.: <sup>14</sup>C reservoir ages show deglacial changes in ocean currents and carbon cycle, *AGU Geophys. Monogr.*, 173, 175–196, 2007.
- Sarnthein, M., Grootes, P. M., Holbourn, A., Kuhnt, W., and Kühn, H.: Tropical warming in the Timor Sea led deglacial Antarctic warming and almost coeval atmospheric CO<sub>2</sub> rise by > 500 yr, *Earth Planet. Sc. Lett.*, 302, 337–348, 2011.

## <sup>14</sup>C reservoir ages and oceanic carbon storage

M. Sarnthein et al.

Title Page

Abstract

Introduction

Conclusions

References

Tables

Figures



Back

Close

Full Screen / Esc

Printer-friendly Version

Interactive Discussion



Schlitzer, R.: Carbon export fluxes in the Southern Ocean: results from inverse modelling and comparison with satellite-based estimates, *Deep Sea Res. Pt. II*, 49, 1623–1644, doi:10.1016/S0967-0645(02)00004-8, 2002.

Schneider, B.: Variable C : N ratios of particulate organic matter and their influence on the marine carbon cycle, *Ber. Z. Polar-Meerforschung.*, 437, 1–98, 2003.

Sigman, D. M. and Boyle, E.: Glacial/interglacial variations in atmospheric carbon dioxide, *Nature*, 407, 859–869, 2000.

Sigman, D. M., Hain, M. P., and Haug, G. H.: The polar ocean and glacial cycles in atmospheric CO<sub>2</sub> concentration, *Nature*, 466, 47–55, 2010.

Sikes, E., Elmore, A., Cook, M., and Guilderson, T.: Depleted Radiocarbon in deep water in the Southwest Pacific and Southern Ocean at the Last Glacial Maximum, in: AGU 2011 Fall Meeting, San Francisco, CA, 5–9 December, abstract PP11B-1784, 2011.

Skinner, L. C.: Glacial-interglacial atmospheric CO<sub>2</sub> change: a possible “standing volume” effect on deep-ocean carbon sequestration, *Clim. Past*, 5, 537–550, doi:10.5194/cp-5-537-2009, 2009.

Skinner, L. C., Fallon, S., Waelbroeck, C., Michel, E., and Barker, S.: Ventilation of the deep Southern Ocean and deglacial CO<sub>2</sub> rise, *Science*, 328, 1147–1151, 2010.

Stommel, H.: Thermohaline convection with two stable regimes of flow, *Tellus*, 13, 224–230, 1961.

Stramma, L., Johnson, G. C., Sprintall, J., and Mohrholz, V.: Expanding oxygen-minimum zones in the tropical oceans, *Science*, 320, 655–658, 2008.

Stuiver, M. and Braziunas, T. V.: Modeling atmospheric <sup>14</sup>C influences and <sup>14</sup>C ages of marine samples to 10 000 BC, *Radiocarbon*, 35, 137–189, 1993.

Svensson, A., Andersen, K. K., Bigler, M., Clausen, H. B., Dahl-Jensen, D., Davies, S. M., Johnsen, S. J., Muscheler, R., Rasmussen, S. O., Röthlisberger, R., Steffensen, J. P., and Vinther, B. M.: The Greenland ice core chronology 2005, 15–42 ka. Part 2: comparison to other records, *Quaternary Sci. Rev.*, 25, 3258–3267, 2006.

Tagliabue, A., Bopp, L., Roche, D. M., Bouttes, N., Dutay, J.-C., Alkama, R., Kageyama, M., Michel, E., and Paillard, D.: Quantifying the roles of ocean circulation and biogeochemistry in governing ocean carbon-13 and atmospheric carbon dioxide at the last glacial maximum, *Clim. Past*, 5, 695–706, doi:10.5194/cp-5-695-2009, 2009.

Takahashi, T., Broecker, W., and Langer, S.: Redfield ratio based on chemical data from isopycnal surfaces, *J. Geophys. Res.*, 90, 6907–6924, 1985.

## <sup>14</sup>C reservoir ages and oceanic carbon storage

M. Sarnthein et al.

Title Page

Abstract

Introduction

Conclusions

References

Tables

Figures

⏪

⏩

◀

▶

Back

Close

Full Screen / Esc

Printer-friendly Version

Interactive Discussion



Thiede, J.: Wind regimes over the late Quaternary southwest Pacific Ocean, *Geology*, 7, 259–262, 1979.

Thornalley, D. J. R., Barker, S., Broecker, W. S., Elderfield, H., and McCave, I. N.: The deglacial evolution of the North Atlantic deep convection, *Science*, 331, 202–205, 2011.

5 Voelker, A.: Zur Deutung der Dansgaard-Oeschger Ereignisse in ultrahoch auflösenden Sedimentprofilen aus dem Europäischen Nordmeer, D.Sc. Thesis, Univ. of Kiel, Kiel, Germany, 1–180, 1999.

Waelbroeck, C., Duplessy, J.-C., Michel, E., Labeyrie, L., Paillard, D., and Duprat, J.: The timing of the last deglaciation in North Atlantic climate records, *Nature*, 412, 724–727, 2001.

10 Yu, J., Broecker, W. S., Elderfield, H., Jin, Z., McManus, J., and Zhang, F.: Loss of carbon from the deep sea since the last glacial maximum, *Science*, 330, 1084–1087, 2010.

Zeebe, R. and Wolf-Gladrow, D.: *CO<sub>2</sub> in Seawater: Equilibrium, Kinetics, Isotopes*, Elsevier, Amsterdam, 2001.

## <sup>14</sup>C reservoir ages and oceanic carbon storage

M. Sarnthein et al.

**Table 1a.** Variability range of shifts in <sup>14</sup>C ventilation age of deep waters vs. today (Matsumoto, 2007) and related shifts in DIC (Fig. 2a), alkalinity (Fig. 4), and CO<sub>3</sub><sup>2-</sup> (in μmol kg<sup>-1</sup>) deduced for the LGM, HS-1, and B/A and various ocean regions below 1500–2000 m w.d. Delta <sup>14</sup>C values (‰) for intra-LGM, intra-HS-1, and intra-B/A age differences between atmosphere and deep-water (calculated from apparent benthic ventilation ages; yr) and related DIC, alkalinity, oxygen, and PO<sub>4</sub> estimates (Figs. 2, 4, and 6), moreover the difference between these Δ<sup>14</sup>C values and their modern correlatives are all calculated for a fraction of “paleo” Modern Carbon (fMC) = 1.0. Using the modern regression slopes characteristic of different regions (based on GLODAP data; Key et al., 2004), we also list average maximum O<sub>2</sub> concentrations and the ratio of PO<sub>4</sub> vs. ventilation age. Records PS2644 and RAPID-10-1P are incorporated from < 1500 m w.d., as these sites match immediate source regions of modern NADW to the north and south of Iceland, except for HS-1, where they record a northward flow of intermediate waters (Fig. 3b). From less than 2000 m w.d. we incorporate records of Site 17940 from 1727 m in the South China Sea, since it is bathed in deep waters entrained from Upper Pacific Deepwater, and Site MD01-7380 from 1787 m depth in the Eastern Indian Ocean, which is bathed in Upper Indian Ocean Deepwater. Because of too low benthic specimen numbers in Core PS2644 the B/A age for the Icelandic Sea is not based on direct dating but on analogies to today, deduced from high local benthic δ<sup>13</sup>C values of 1.1–1.4‰ (Voelker, 1999), thus earmarked by a question mark in Fig. 3a.

[Title Page](#)[Abstract](#)[Introduction](#)[Conclusions](#)[References](#)[Tables](#)[Figures](#)[Back](#)[Close](#)[Full Screen / Esc](#)[Printer-friendly Version](#)[Interactive Discussion](#)

**<sup>14</sup>C reservoir ages and oceanic carbon storage**

M. Sarnthein et al.

**Table 1a.** Caption on previous page.

SHIFT in ventilation age vs. today (x yr = -yr ‰ <sup>14</sup> C)	SHIFT in DIC (μmol C kg <sup>-1</sup> ) (yr ‰ <sup>14</sup> C × gradient)	SHIFT in ALKALINITY (yr ‰ <sup>14</sup> C × gradient)	SHIFT in CO <sub>3</sub> <sup>2-</sup> concentr. (μmol C kg <sup>-1</sup> ) (Alkalinity–DIC)	Deep water O <sub>2</sub> max. values (μmol O <sub>2</sub> kg <sup>-1</sup> )	PO <sub>4</sub> vs. ventilation age (slope gradient)
Icelandic Sea <sup>(a)</sup> (modern vent. age: 550 yr)			(modern CO <sub>3</sub> <sup>2-</sup> : 100–105)	Today: 241– –x ‰ × –0.71 =)	
LGM: +1450–+2000 yr = –165––220 ‰	x –1.49 = +246/+328	x –1.15 = +190/+253	–56/–75	124/85	x –0.01
LGM: –180––110 yr = +23–+14 ‰	x –1.49 = –34/–21	x –1.15 = –26/–16	+8/+5	257/251	x –0.01
HS-1: +700–+1400 yr = –83––160 ‰	x –1.49 = +123/+238	x –1.15 = +95/+184	–28/–54	182/127	x –0.01
B/A: 0 yr = 0 ‰	x –1.49 = 0	x –1.15 = 0	0	241	x –0.01
Northeastern North Atlantic <sup>(b)</sup> (modern vent. age: 600 yr)			(modern CO <sub>3</sub> <sup>2-</sup> : 100–105)	Today: 241– –x ‰ × –0.71 =)	
LGM: +1800–+2000 yr = –201––220 ‰	x –1.49 = +300/+317	x –1.15 = +231/+253	–69/–64	98/85	x –0.01
HS-1: +4000–+4500 yr = –392––429 ‰	x –1.49 = +584/+639	x –1.15 = +451/+493	–133/–146	0	x –0.01
B/A: 0––1000 yr = 0–+117 ‰	x –1.49 = 0/–174	x –1.15 = 0/–135	0/–39	241/158	x –0.01
Western North Atlantic <sup>(c)</sup> (modern vent. age: 700 yr)			(modern CO <sub>3</sub> <sup>2-</sup> : 100–105)	Today: 241– –x ‰ × –0.71 =)	
HS-1: +500–+1700 yr = –60––191 ‰	x –1.49 = +89/+285	x –1.15 = +69/+220	–20/–65	198/105	x –0.01
Southern Ocean (Atlantic sector) <sup>(d)</sup> (modern vent. age: 1200 yr)			(modern CO <sub>3</sub> <sup>2-</sup> : 80)	Today: 226– –x ‰ × –1.26 =)	
LGM: +1600–+3100 yr = –181––320 ‰	x –1.43 = +259/+458	x –1.06 = +192/+339	–67/–119	0	x –0.02
HS-1: +700–+2400 yr = –83––258 ‰	x –1.43 = +119/+369	x –1.06 = +88/+273	–31/–96	121/0	x –0.02
B/A: –300–+1000 yr = +37––117 ‰	x –1.43 = –53/+167	x –1.06 = –39/+124	–14/–43	273/79	x –0.02

<sup>a</sup>End members of oscillating deepwater regimes.

Title Page

Abstract Introduction

Conclusions References

Tables Figures

◀ ▶

◀ ▶

Back Close

Full Screen / Esc

Printer-friendly Version

Interactive Discussion



**<sup>14</sup>C reservoir ages and oceanic carbon storage**

M. Sarnthein et al.

**Table 1a.** Continued.

SHIFT in ventilation age vs. today ( $x$ yr = $-y$ ‰ $^{14}\text{C}$ )	SHIFT in DIC ( $\mu\text{mol C kg}^{-1}$ ) (yr‰ $^{14}\text{C} \times$ gradient)	SHIFT in ALKALINITY (yr‰ $^{14}\text{C} \times$ gradient)	SHIFT in $\text{CO}_3^{2-}$ concentr. ( $\mu\text{mol C kg}^{-1}$ ) (Alkalinity–DIC)	Deep water $\text{O}_2$ max. values ( $\mu\text{mol O}_2 \text{ kg}^{-1}$ )	$\text{PO}_4$ vs. ventilation age (slope gradient)
Eastern Indian Ocean <sup>(6)</sup> (modern vent. age: 1950 yr)			(modern $\text{CO}_3^{2-}$ : 84)	Today: 174– $-x$ ‰ $\times -1.7$ =)	
LGM: +50––500 yr = –6–+64 ‰	$\times -1.27 = +8/-81$	$\times -1.18 = +7/-76$	–1/+5	164/283	$\times -0.0075$
HS-1: –200––100 yr = +25–+13 ‰	$\times -1.27 = -32/-17$	$\times -1.18 = -30/-15$	+2/+2	216/196	$\times -0.0075$
B/A: –300––500 yr = +37–+64 ‰	$\times -1.27 = -47/-81$	$\times -1.18 = -44/-76$	+3/+5	237/283	$\times -0.0075$
South China Sea <sup>(1)</sup> (modern vent. age: 1900 yr)			(modern $\text{CO}_3^{2-}$ : 73)	Today: 141– $-x$ ‰ $\times -1.68$ =)	
LGM: +1100–+2350 yr = –130––254 ‰	$\times -1.44 = +187/+366$	$\times -0.96 = +125/+244$	–62/–122	0	$\times -0.009$
HS-1: –550––1500 yr = +71–+205 ‰	$\times -1.44 = -102/-295$	$\times -0.96 = -68/-197$	+34/+98	260/485	$\times -0.009$
B/A: –1100––400 yr = +130–+50 ‰	$\times -1.44 = -187/-72$	$\times -0.96 = -125/-48$	+62/+24	360/225	$\times -0.009$
Northwest Pacific Ocean <sup>(9)</sup> (modern vent. age: 2100 yr)			(modern $\text{CO}_3^{2-}$ : 73)	Today: 141– $-x$ ‰ $\times -1.68$ =)	
LGM: +850–+1000 yr = –100––117 ‰	$\times -1.44 = +144/+168$	$\times -0.96 = +96/+112$	–48 /–56	0	$\times -0.009$
HS-1: GAP	–	–	–	–	–
B/A: +1000––500 yr = –117–+64 ‰	$\times -1.44 = +168/-92$	$\times -0.96 = +112/-61$	–56/+31	0/249	$\times -0.009$
Northeast Pacific Ocean <sup>(11)</sup> (modern vent. age: 2200 yr)			(modern $\text{CO}_3^{2-}$ : 73)	Today: 141– $-x$ ‰ $\times -1.68$ =)	
LGM: +300 yr = –37 ‰	$\times -1.44 = +53$	$\times -0.96 = +36$	–17	79	$\times -0.009$
HS-1: –1150–+300 yr = +154––37 ‰	$\times -1.44 = -222/+53$	$\times -0.96 = -148/+36$	+74/–17	400/79	$\times -0.009$
B/A: +200––750 yr = –25–+98 ‰	$\times -1.44 = -36/+141$	$\times -0.96 = -24/+94$	+12/–47	99/306	$\times -0.009$
Southern Ocean (Pacific Sector) TODAY			(modern $\text{CO}_3^{2-}$ : 79)	(Today: 193)	$\times -0.0048$
	$\times -0.79$	$\times -0.83$	–	–	

Title Page

Abstract

Introduction

Conclusions

References

Tables

Figures

◀

▶

◀

▶

Back

Close

Full Screen / Esc

Printer-friendly Version

Interactive Discussion



**<sup>14</sup>C reservoir ages  
and oceanic carbon  
storage**

M. Sarnthein et al.

**Table 1b.** List of core locations (compare Fig. 3) and techniques #1–5 used to obtain benthic reservoir ages and shortly explained in the Methods section, and published data sources. Reservoir ages derived by technique #5 were modified on the basis of slight shifts in <sup>14</sup>C plateau boundary ages identified in the new “Suigetsu” atmospheric <sup>14</sup>C record (Ramsey et al., 2012). – Apparent ventilation ages and data sources listed in Table 1 and Fig. 3 are deposited at PANGAEA databank (<http://www.pangaea.de/PangaVista>).

CORE NUMBER	LOCATION	published by	ABSOLUTE CHRONOLOGY deduced by
(a) PS2644	67°52′ N, 21°46′ W, 777 m w.d.	Sarnthein et al. (2007), suppl. by unpubl. data	Technique # 5
(b) RAPiD-10-1P	62°59′ N, 17°35′ W, 1237 m w.d.	Thornalley et al. (2011)	Technique # 3 plus # 4
RAPiD-15-4P	62°18′ N, 17°08′ W, 2133 m w.d.	Thornalley et al. (2011)	
RAPiD-17-5P	61°29′ N, 19°32′ W, 2303 m w.d.	Thornalley et al. (2011)	
MD99-2334	37°48′ N, 10°10′ W, 3146 m w.d.	Skinner et al. (2010)	
(c) Coral transects	33°30′–39°0′ N, 60°30′–62°30′ W, 1700–2300 m w.d.	Robinson et al. (2005)	Technique # 1
(d) TNO57-21	41°06′ S, 7°48′ E, 4981 m w.d.	Barker et al. (2010)	Technique # 2
MD07 3076	44°05′ S, 14°13′ W, 3770 m w.d.	Skinner et al. (2010)	Technique # 4
(e) MD01-2378	13°05′ S, 123° 43.3′ E, 1783 m w.d.	Sarnthein et al. (2011)	Technique # 5
(f) GIK 17940	27°07′ N, 117°23′ E, 1727 m w.d.	Sarnthein et al. (2007), suppl. by unpubl. data	Technique # 5
	(record of Pacific inflow waters entraining upper Pacific deep waters)		
(g) MD01-2416	51°27′ N, 167°73′ E, 2317 m w.d.	Sarnthein et al. (2007)	Technique # 5
MD98-2181	6°18′ N, 125°49′ E, 2114 m w.d.	Broecker et al. (2004), suppl. by unpubl. data	Synsedimentary wood chunks and planktic foraminifera
(h) MD02-2489	54°39′ N, 148°92′ W, 3640 m w.d.	Gebhardt et al. (2008), corroborated by unpubl. Supplement	Technique # 5

Title Page

Abstract

Introduction

Conclusions

References

Tables

Figures



Back

Close

Full Screen / Esc

Printer-friendly Version

Interactive Discussion



**$^{14}\text{C}$  reservoir ages  
and oceanic carbon  
storage**

M. Sarnthein et al.

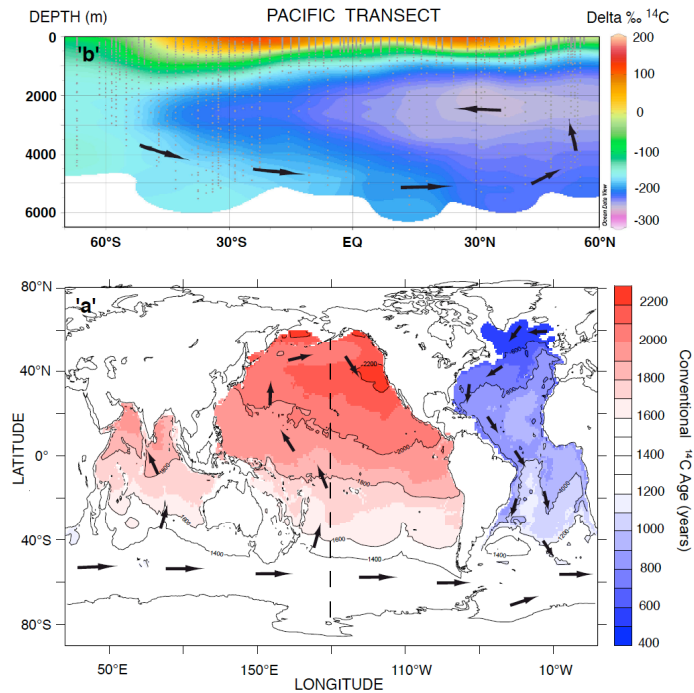


**Fig. 1.** Modern apparent ventilation ages based on natural radiocarbon in the ocean below 1500 m w.d (a) (Matsumoto, 2007, modified). Arrows indicate long-term directions of circulation. Broken line = transect position. (b) North-south transect across Pacific at 160° W (based on GLODAP data; Key et al., 2004).

**<sup>14</sup>C reservoir ages and oceanic carbon storage**

M. Sarnthein et al.

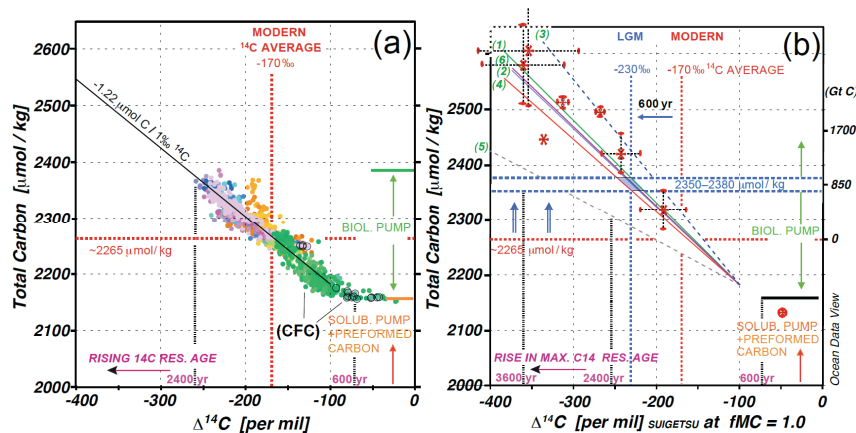


Fig. 2. Caption on next page.

Title Page

Abstract

Introduction

Conclusions

References

Tables

Figures

⏪

⏩

◀

▶

Back

Close

Full Screen / Esc

Printer-friendly Version

Interactive Discussion



## <sup>14</sup>C reservoir ages and oceanic carbon storage

M. Sarnthein et al.

**Fig. 2. (a)** Ratio of total dissolved inorganic carbon (DIC) per kg seawater vs. benthic <sup>14</sup>C reservoir (ventilation) age for fMC = 1 of ocean waters below > 2000 m w.d. **(a)** Modern GLODAP data (Key et al., 2004) for longitudes of the Atlantic (green), the western (orange) and eastern Indian Ocean and Pacific (pink and blue). Black open circles mark deep waters with chlorofluorocarbon (CFC) concentrations > 0.1 pmol kg<sup>-1</sup> as tracer of modern anthropogenic influence in the northern North Atlantic and Weddell Sea Bottom Water (orange dots). Modern ventilation ages of 600 to 2400 yr average at 1500 yr = -170‰. **(b)** Variability of modern DIC–age ratio for six major ocean regions (green numbers at upper left) defined in Fig. 5. Regressions slopes are -1.48 μmol kg<sup>-1</sup> (1), -1.43 μmol kg<sup>-1</sup> (2), -1.87 μmol kg<sup>-1</sup> (3), -1.27 μmol kg<sup>-1</sup> (4), -0.79 μmol kg<sup>-1</sup> (5), -1.44 μmol kg<sup>-1</sup> (6). Red asterisks depict LGM regional estimates and variability ranges of DIC–ventilation age ratio. Following Fig. 2a, Δ<sup>14</sup>C values for intra-LGM age differences between atmosphere and deep-water (= apparent benthic ventilation ages) and related DIC values are calculated for “paleo” fMC = 1 (Table 1). LGM ventilation ages show end members of 600 yr in the Icelandic Sea and 3600 yr in both the Southern Ocean and Northwest Pacific, resulting in an average of 2100 yr equal to -230‰ of fMC. 4400 yr occur in the South China Sea (S.C.S.) segregated from the open ocean. Blue numbers (μmol kg<sup>-1</sup>) show mean DIC stored in the ocean (excluding the South China Sea), estimated for a mean LGM ventilation age of 2100 yr. Gt C scale at upper right labels DIC mass in the LGM ocean, stored in addition to the modern 38 100 Gt DIC, with 1 μmol DIC kg<sup>-1</sup> corresponding to 8.5 Gt C in the total ocean at > 2000 m w.d. (deep-sea morphology of Amante and Eakins, 2009). Biol. Pump = “Biological Pump”, Solub. Pump = “Solubility Pump”.

Title Page

Abstract

Introduction

Conclusions

References

Tables

Figures

⏪

⏩

◀

▶

Back

Close

Full Screen / Esc

Printer-friendly Version

Interactive Discussion



**$^{14}\text{C}$  reservoir ages  
and oceanic carbon  
storage**

M. Sarnthein et al.

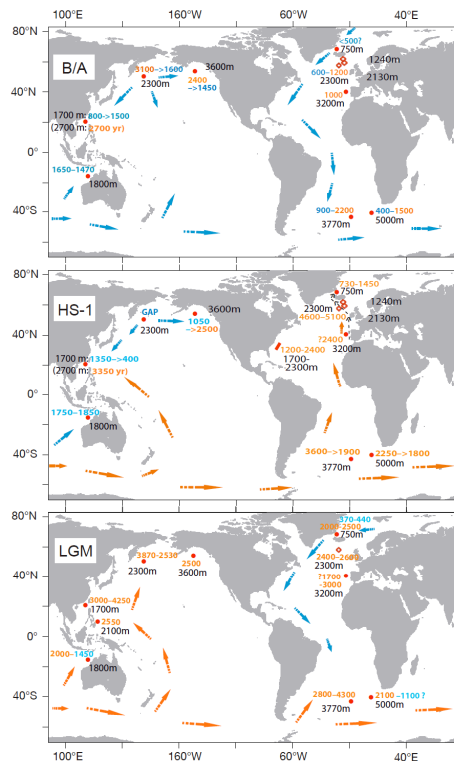


**Fig. 3.** Ranges of past  $^{14}\text{C}$  ventilation ages and simplified circulation patterns below 1500 m w.d. (Sarnthein, 2011, modified; arrows inferred per analogy to Fig. 1) for the Bølling-Allerød (B/A), Heinrich-Stadial 1 (HS-1), and Last Glacial Maximum (LGM). Core locations and published data sources are listed in Table 1. Orange numbers and arrows mark waters with ventilation ages higher than today, blue numbers and arrows present waters with ages equal or lower than today (Fig. 1). Question marks earmark age estimates based on disputable dating techniques and/or indirect evidence (Table 1b and Supplement Sect. 2). Hatched black arrows mark potential current of intermediate waters during HS-1.

Title Page

Abstract

Introduction

Conclusions

References

Tables

Figures



Back

Close

Full Screen / Esc

Printer-friendly Version

Interactive Discussion



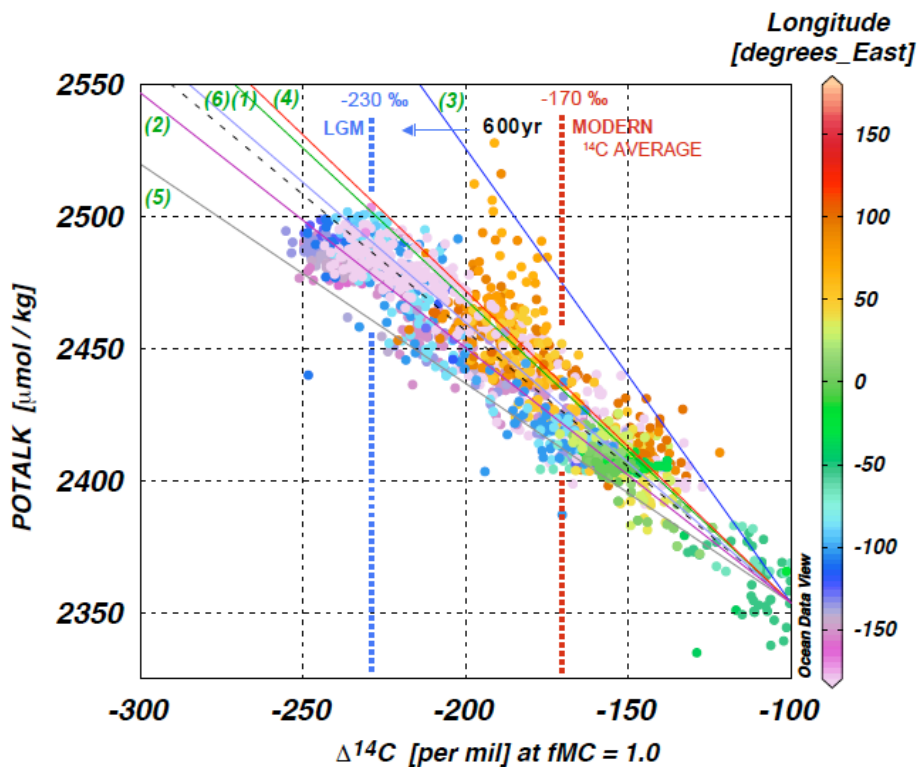


**Fig. 4.** Modern regression slopes of  $\Delta^{14}\text{C}$  vs. potential alkalinity (POTALK) in ocean waters below 2000 m w.d., based on GLODAP data (Key et al., 2004), showing the differential influence of deep-ocean calcite dissolution on total alkalinity in six major ocean regions (green numbers at upper left refer to regions displayed in Fig. 5). Global average regression line is hatched. Color scale indicates eastern longitudes of deep waters. Vertical dotted lines mark modern and LGM average ventilation ages of 1500/2100 yr.

**$^{14}\text{C}$  reservoir ages and oceanic carbon storage**

M. Sarnthein et al.

Title Page

Abstract

Introduction

Conclusions

References

Tables

Figures

⏪

⏩

◀

▶

Back

Close

Full Screen / Esc

Printer-friendly Version

Interactive Discussion



## $^{14}\text{C}$ reservoir ages and oceanic carbon storage

M. Sarnthein et al.

Title Page

Abstract

Introduction

Conclusions

References

Tables

Figures



Back

Close

Full Screen / Esc

Printer-friendly Version

Interactive Discussion

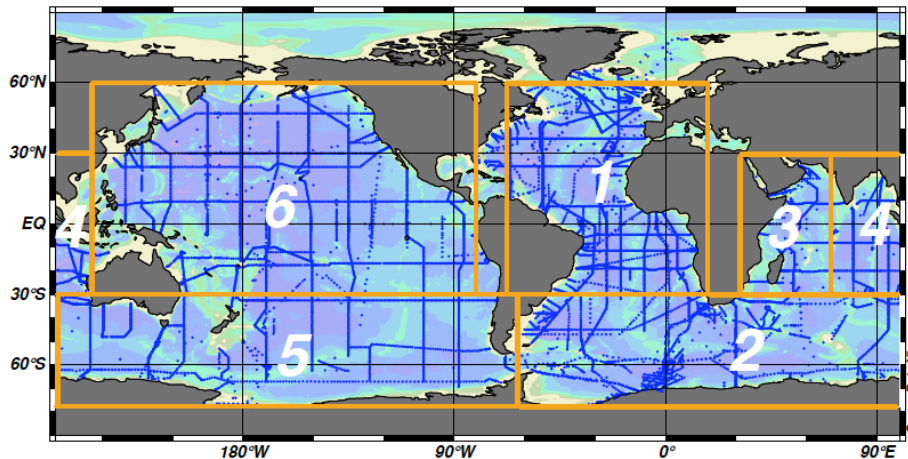


**Fig. 5.** Six major ocean regions used for testing the uncertainty range of the relationships of DIC and total alkalinity vs. age (at  $>2000$  m w.d.). To the north region 3 ends in a monsoon-driven belt of high upwelling productivity off Somalia and southern Arabia. Region 5 includes the low-productive subtropical and subpolar southern Pacific ocean.

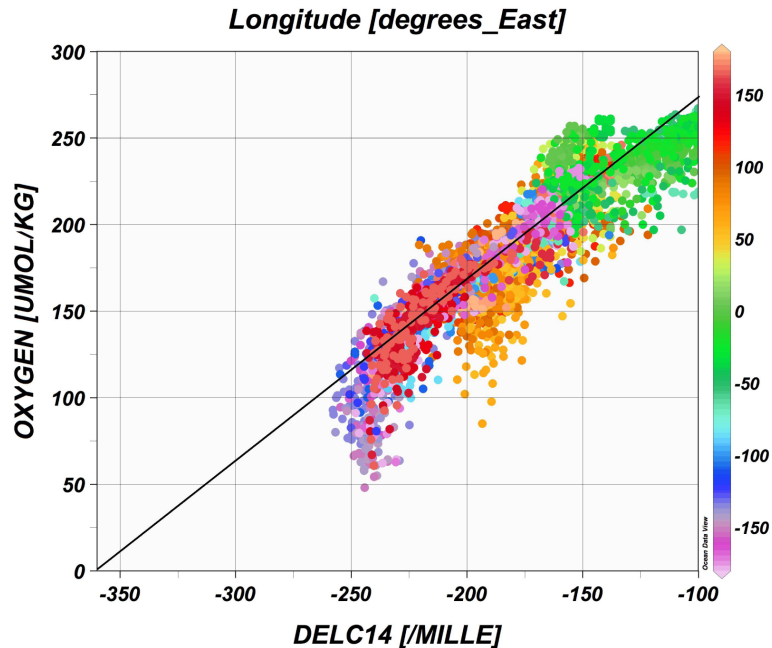


**Fig. 6.** Ratio of total dissolved oxygen ( $\mu\text{mol O}_2$ ) per kg seawater vs.  $^{14}\text{C}$  reservoir (ventilation) age in the modern ocean below  $> 2000$  m w.d. Positive  $\text{O}_2$  “bump” at  $-140$  to  $-170$  per mil  $^{14}\text{C}$  reflects the advection of freshly ventilated Weddell Sea waters. The regression line extrapolated down to  $-360$  per mil  $^{14}\text{C}$  (i.e. to the maximum LGM deep-water age shown in Fig. 3) depicts the maximum  $\text{O}_2$  averaged for each per mil of deep-water  $^{14}\text{C}$  ventilation ages, that is for organic carbon flux rates below low-productivity regions. Enhanced  $\text{O}_2$  depletion at  $-175$  to  $-200$  and  $-225$  to  $-250$ ‰  $\Delta^{14}\text{C}$  reflects increased flux rates of organic carbon below high productivity zones in the northern Indian and Pacific oceans each.

**$^{14}\text{C}$  reservoir ages and oceanic carbon storage**

M. Sarnthein et al.

Title Page

Abstract Introduction

Conclusions References

Tables Figures

⏪ ⏩

⏴ ⏵

Back Close

Full Screen / Esc

Printer-friendly Version

Interactive Discussion

